



*For inspection purposes only.  
Consent of copyright owner required for any other use.*

# **SSE Great Island CCGT**

Modelling Report

16 July 2020

For inspection purposes only.  
Consent of copyright owner required for any other use.

Mott MacDonald  
South Block  
Rockfield  
Dundrum  
Dublin 16  
D16 R6V0  
Ireland

T +353 (0)1 2916 700  
mottmac.com

*For inspection purposes only.  
Consent of copyright owner required for any other use.*

SSE Generation Ireland  
Great Island CCGT  
Campile  
New Ross  
Co. Wexford  
Ireland  
Y34 KC62

# **SSE Great Island CCGT**

## **Modelling Report**

16 July 2020

Directors: J T Murphy BE HDipMM CEng  
FIEI FConsEI FIAE (Managing), D Herlihy  
BE MSc CEng, R Jefferson BSc MSCS  
MRICS MCI Arb DipConLaw, J Shinkwin  
BE DipMechEng CEng MIEI, M D Haigh  
BSc CEng FICE MCIWEM (British)  
Innealtóirí Comhairleach (Consulting  
Engineers)  
Company Secretary: Michael Cremin CPA  
Registered in Ireland no. 53280.  
Mott MacDonald Ireland Limited is a  
member of the Mott MacDonald Group

For inspection purposes only.  
Consent of copyright owner required for any other use.

# Issue and Revision Record

Revision	Date	Originator	Checker	Approver	Description
A	31/01/2020	DP/RA/RB	MMDA/NR	JJW	Revision A for comments
B	12/02/20	DP/RA/RB	MMDA/NR	JJW	Revision B for information
C	16/07/2020	DP/RA/RB	RM/NR/ MMDA	JJW	Revision C including draft EPA comments

**Document reference:** 414088 | 001 | C

**Information class:** Standard

This document is issued for the party which commissioned it and for specific purposes connected with the above-captioned project only. It should not be relied upon by any other party or used for any other purpose.

We accept no responsibility for the consequences of this document being relied upon by any other party, or being used for any other purpose, or containing any error or omission which is due to an error or omission in data supplied to us by other parties.

This document contains confidential information and proprietary intellectual property. It should not be shown to other parties without consent from us and from the party which commissioned it.

For information purposes only.  
Consent of copyright owner required for any other use.

# Contents

Executive summary	1
<b>1 Introduction</b>	<b>4</b>
1.1 Project background	4
1.2 Report structure	5
<b>2 Modelling approach</b>	<b>6</b>
2.1 Introduction	6
<b>3 Hydrodynamic model setup</b>	<b>7</b>
3.1 Data	7
3.1.1 Bathymetry	7
3.1.2 Water levels	7
3.1.3 Tidal current speed and direction	7
3.1.4 Temperature and salinity	8
3.2 Model setup	9
3.2.1 Horizontal and vertical references	9
3.2.2 Model mesh and extent	9
3.2.3 Vertical mesh	11
3.2.4 Model bathymetry	12
3.2.5 Boundary conditions	13
3.2.6 Bed roughness	13
3.2.7 Eddy viscosity	14
3.2.8 Dispersion	14
3.2.9 River flows	15
<b>4 Hydrodynamic model calibration and validation</b>	<b>16</b>
4.1 Hydrodynamic Model Calibration	16
4.2 Performance Criteria	16
4.3 Calibration results	17
4.3.1 Water level	17
4.3.2 Tidal current speed and direction	20
4.4 Model validation	21
4.4.1 Water level	21
4.4.2 Tidal currents	24
<b>5 Chlorine dispersion modelling</b>	<b>26</b>
5.1 Introduction	26
5.2 Boundary and outfall configuration in the model	26

5.3	Sensitivity to chlorine decay	28
5.4	Initial test of model performance	28
5.5	Neap tide simulation	29
5.6	Field data collection and analysis	34
<b>6</b>	<b>Modelling pH</b>	<b>36</b>
6.1	Introduction	36
6.2	Model setup	37
6.3	pH results	38
6.3.1	Spatial distribution	38
6.3.2	Temporal distribution	39
<b>7</b>	<b>Biological Effects</b>	<b>44</b>
7.1	Characteristics of NaOCl in the marine environment	44
7.2	Ecology of Barrow Estuary	45
7.2.1	Site designations and features of conservation importance	45
7.2.2	Estuarine benthic ecology	46
7.3	Literature review of chlorinated effluent impacts on ecological receptors	47
7.3.1	Plankton	47
7.3.2	Fish	50
7.3.3	Mammals	51
7.3.4	Birds	51
7.4	Assessment of the potential impacts of chlorinated effluent on ecological receptors in Barrow Estuary	52
<b>8</b>	<b>Environmental Impacts</b>	<b>54</b>
8.1	Barrow Estuary	54
8.1.1	NaOCl	54
8.1.2	pH	54
8.1.3	Bioassays	54
8.1.4	Biological Environment	55
8.1.5	Overall Benthic Community Habitat	56
8.1.6	Indicators of Impacts Caused by the Outflow Plume	57
8.1.7	Wild birds	58
8.1.8	Fish Species	59
8.1.9	Mammal Species	60
<b>9</b>	<b>Conclusions</b>	<b>61</b>
	<b>References</b>	<b>63</b>
	<b>Appendices</b>	<b>66</b>

For inspection purposes only.  
Consent of copyright owner required for any other use.

## A. Water sampling campaign II

67

### Tables

Table 4.1: Statistical guidelines to establish calibration standards for a minimum level of performance for coastal and estuarine hydrodynamic models	17
Table 4.2: Spring tide error statistics for water levels	20
Table 4.3: Neap tide model validation performance statistics for water levels	24
Table 4.4: Spring and neap tide error statistics for current speeds	25
Table 5.1: Results from the measurements at sites A, B and C on 28 <sup>th</sup> Jan 2020	35
Table 6.1: pH model inputs	38
Table 7.1.: River Barrow and River Nore SAC habitats listed under Annex I of the EU Habitats Directive (* = priority)	45
Table 7.2: River Barrow and River Nore SAC species listed under Annex II of the EU Habitats Directive	45
Table 7.3: River Barrow and River Nore SAC birds listed under Article 4 of the EU Birds Directive	46

### Figures

Figure 1.1: Location of the Great Island Combined Cycle Gas Turbine (CCGT) power station	4
Figure 3.1: Location of observation water level and current speed data (SN076C tidal diamond)	8
Figure 3.2: EPA salinity measurements (surface and bed) compared against upstream river flow at Graiguenamanagh	9
Figure 3.3: MIKE3 FM HD overall model mesh and approximate mesh resolution	10
Figure 3.4: MIKE3 FM HD model mesh in the vicinity of the Great Island Power Station and approximate mesh resolution	11
Figure 3.5: MIKE3 FM HD model bathymetry of entire domain	12
Figure 3.6: Model bathymetry in the vicinity of the project site	12
Figure 3.7: Bed roughness length as used in the model	14
Figure 4.1: Spring tide comparisons between observed (black) and simulated (red) water levels	18
Figure 4.2: Spring tide comparisons between observed (black) and simulated (red) water levels	19
Figure 4.3: Spring tide current speed and direction comparison: black (observed), red (model)	20
Figure 4.4: Neap tide comparisons between observed (black) and simulated (red) water levels	21
Figure 4.5: Neap tide comparisons between observed (black) and simulated (red) water levels	23
Figure 4.6: Neap tide current speed and direction model validation comparison: black (observed), red (model)	24



Figure 5.1: Temperature increase from intake to outfall	27
Figure 5.2: Free Chlorine concentration in the outfall discharge (mg/l)	28
Figure 5.3: Visual comparison between aerial imagery and the model prediction of the cooling water outfall plume during the latter stages of the ebb tide	29
Figure 5.4: Bottom Layer: maximum chlorine concentrations (mg/l) throughout neap tides	30
Figure 5.5: Surface Layer: maximum chlorine concentrations (mg/l) throughout neap tides	30
Figure 5.6: Bottom layer: percentage of time chlorine concentration exceeds 0.05mg/l	31
Figure 5.7: Bottom layer: percentage of time chlorine concentration exceeds 0.1mg/l	32
Figure 5.8: Bottom layer: percentage of time chlorine concentration exceeds 0.2mg/l	32
Figure 5.9: Surface layer: percentage of time chlorine concentration exceeds 0.05mg/l	33
Figure 5.10: Surface layer: percentage of time chlorine concentration exceeds 0.1mg/l	33
Figure 5.11: Surface layer: percentage of time chlorine concentration exceeds 0.2mg/l	34
Figure 6.1: Measured pH at the power station outfall, and water level at Kilmokea for the period November to December 2019	36
Figure 6.2: Measured pH at the power station outfall, EPA measurements of pH and river flows at Graiguenamanagh	37
Figure 6.3: EPA measured pH values upstream of New Ross and river flows at Graiguenamanagh	37
Figure 6.4: Source locations in the pH modelling study	38
Figure 6.5: Spatial pH variation in the surface layer during high water level near the power station outfall.	39
Figure 6.6: Spatial pH variation in the surface layer during low water level near the power station outfall.	39
Figure 6.7: Overview of pH variation at bottom layer during high water level.	40
Figure 6.8: Overview of pH values at bottom layer during low water level.	40
Figure 6.9: pH values at A and C at the surface and bottom layer.	41
Figure 6.10: Maximum short-term pH values at surface layer.	42
Figure 6.11: Maximum short-term pH values at bottom layer.	42
Figure 6.12: EPA pH measurements at three locations close to the Great Island Power Station	43
Figure 8.1: Location of 7 Sample Stations (Aquafact 2020)	55
Figure 8.2: Location of Intertidal Transects (Aquafact 2020)	56

# Glossary

CCGT	Combined Cycle Gas Turbine
CPO	Chlorine-Produced Oxidants
DEM	Digital elevation model
EPA	Environment Protection Authority
FM	Flexible Mesh
Free chlorine	Residual chlorine in water present as dissolved gas ( $\text{Cl}_2$ ), hypochlorous acid ( $\text{HOCl}$ ), and/or hypochlorite ion ( $\text{OCl}^-$ )
DHI	Danish Hydraulic Institute
DT50	Half-life defined as the time it takes for an amount of a compound to be reduced by half through degradation
HD	Hydrodynamic
IED	Industrial Emissions Directive
LC50	Lethal Concentration 50% - the concentration at which 50% of the individuals are expected to die
LC90	Lethal Concentration 90% - the concentration at which 90% of the individuals are expected to die
LOEC	Lowest Observed Effect Concentration – lowest concentration in an environmental compartment that has a statistically significant adverse effect on exposed organisms compared with controls
MIKE3	DHI numerical modelling software
NOEC	No Observed Effect Concentration – the concentration in an environmental compartment (water, soil, etc.) below which an unacceptable effect is unlikely to be observed
ODM	Ordinance Datum Malin
OPW	Office of Public Works
pH	Potential of hydrogen
PSU	Practical salinity unit
$R^2$	Pierson product moment correlation coefficient
RMSE	Root mean square error
SAC	Special area of conservation
TRO	Total Residual Oxidant
TLm	Median Tolerance Limit – the concentration in water at which 50% of the individuals are able to survive for a particular period of exposure
TRC	Total Residual Chlorine

# Executive summary

SSE Generation Ireland Limited operates a 430MW output natural gas fired Combined Cycle Gas Turbine (CCGT) power plant at Great Island, County Wexford under IED Licence Reg. No. P0606-03.

As part of the process, water is abstracted from the River Barrow as cooling water used in the steam turbine condenser. Sodium hypochlorite is added at the cooling water intake, the purpose of which is to prevent the biological fouling of the heat exchangers in the steam turbine condenser. Following this the cooling water is discharged back into the River Barrow via a spillway. The Industrial Emissions Licence (IED) gives an emissions limit in this discharge of 0.3 mg/l chlorine. The discharge remains compliant with the IED Licence which permits chlorine in the cooling water discharge to a maximum concentration of 0.3mg/l at the cooling water outlet.

The Environmental Protection Agency, as Competent Authority for the IED licence, has requested an assessment of the effects of sodium hypochlorite use at the plant on the receiving environment in the Barrow Estuary.

This report is a desk-based assessment of the likely impact(s) of the cooling water discharge on the receiving environment in the Barrow Estuary (biological, chemical and physical) under current sodium hypochlorite usage.

Physical and chemical processes have been investigated using a calibrated three-dimensional (3D) hydrodynamic (HD) model of the Barrow Estuary to simulate the tidal flows and fluvial inputs.

The potential biological effects of the discharge are assessed through a desk-based literature review, subtidal benthic assessment and intertidal survey within the Barrow Estuary, and toxicity analysis of the cooling water discharge.

## **Hydrodynamic Model**

The model accounts for the temperature differences between the cooling water discharge and the receiving water body as well as the temporal and spatial salinity distribution within the estuary. The model is therefore suitable for simulating the physical behaviour of the cooling water plume and the spatial and temporal changes in NaOCl concentrations and pH brought about by mixing and dispersion in the Barrow Estuary. A chlorine tracer was released in the model at the power station outfall to represent the NaOCl discharge. Model runs to simulate the dispersion of the discharge plume and to provide concentrations of NaOCl and water pH both spatially and temporally have been undertaken during neap tidal flow conditions.

In all regards the modelling approach has been conservative to represent as far as practicable potential worst-case scenarios. Model results for NaOCl concentrations and pH have been used to assess the environmental impacts of the cooling water discharge into the Barrow Estuary.

Informed by results from numerical modelling of the mixing zone around the cooling water outflow, and a literature review of the effects of NaOCl in the marine environment, this study draws the following conclusions with regards to the most likely environmental impacts of the cooling water discharge on the Barrow Estuary. However, it has to be noted that this assessment focuses only on the potential environmental impacts of the warm, weakly chlorinated power station outfall discharge. Consideration to other sources of chlorine in the Barrow Estuary from a wide range of domestic, industrial, agricultural and natural sources was outside the present scope.

- Measurements of free chlorine in the power station outfall discharge obtained over a period of 50 months shows that typically concentrations are around 0.2mg/l. While peak free chlorine values reach 0.3mg/l for short periods, the discharge remains compliant with the Industrial Emissions Directive (IED) Licence which permits chlorine in the cooling water discharge to a maximum concentration of 0.3mg/l at the cooling water outlet;
- The modelling approach in the study has been conservative and representative of the worst-case scenarios. It has purposefully:
  - a. excluded natural free chlorine decay;
  - b. assumed zero horizontal dispersion;
  - c. considered only neap tides when advection is low;
  - d. assumed a 10°C excess temperature for the outfall discharge water resulting in high plume buoyancy, less vertical mixing and higher surface free chlorine values; and
  - e. assumed the concentration of free chlorine in the outfall discharge water was 0.3mg/l, a value 0.1 mg/l greater than the mean concentration measured over a period of 50 months;
- Evidence from the MIKE3 NaOCl discharge modelling shows that the concentration of chlorine released from the cooling water outfall falls rapidly from the discharge location due to effective dispersion and dilution in the estuarine water. Concentration of free chlorine around 0.2 mg/l are only likely to be found within 100m of the discharge point for short period during the tidal cycle. It is noted that the model assumes there is no decay in total free chlorine and therefore the actual concentrations in the receiving environment are likely to be lower when considering the known half-life of NaOCl (i.e. less than one minute when in contact with bed sediments and the suspended sediment load of estuarine water);
- The area influenced by the discharge of around 0.2 mg/l constitutes only a very small proportion of the River Barrow and River Nore SAC (~0.02%) and together with tidal flushing, the exposure time for sensitive species within the water column is likely to be limited. Consequently, the direct and indirect impacts of habitats and species of community importance such as finfish and birds within the SAC is also likely to be negligible;
- The MIKE3 NaOCl discharge modelling shows that the chlorine concentrations of 0.1mg/l in the outfall plume can move up to 2km downstream from the outfall in the worst-case; this is caused by a ponding of the cooling water at high water which then moves downstream as a pool whilst mixing with the surrounding water. However, these concentration values occur for less than 2% of the time during a neap tide (<15 minutes) and are confined close to the eastern shore to the estuary where interactions with the sediments will rapidly reduce concentrations (not included in the model). As the ebb tide reaches its peak the pond of water has dispersed and a plume with lower concentrations is formed, with the 0.1mg/l contour only reaching 300m downstream;
- Evidence from the MIKE3 pH modelling show that maximum pH values of 8 occur temporary during periods of slack water during the tidal cycle. The spatial extent of water with a pH of 8 is confined to less than 100m from the outfall location and persists for only a short time during slack water. Subsequent ebb or flood tidal flows rapidly disperse the flume and reduce the pH to values close to the ambient estuarine water values; and
- While the pH of the estuarine water is modified slightly by the outfall discharge, the effects are confined to a region very close to the outfall, and values are sufficiently close to measured values in the wider estuary to suggest any reasons for concern with regards to impacts on the environment.

The literature review found varying degrees of sensitivity to NaOCl and chlorine byproducts which would be associated with the outflow. The variance in sensitivity depends on the species type,

the life stage of a particular species, length of exposure to concentrations, and the concentration of the substances.

Surveys carried out to examine the aquatic ecology in terms of benthic communities found no change in the overall community present when compared to studies carried out in 2008 to support National Parks and Wildlife Service studies. The studies found that subtidal benthic communities showed no statistical difference when compared in close proximity and at a distance from the outflow. A slight difference was found in the intertidal communities, however this was limited to the area directly adjacent to the outflow. The phytoplankton survey found that communities composition was homogenous throughout the estuary. The ecological survey report findings mirror those of the modelling, indicating that the plume disperses quickly and effects are limited to directly surrounding the outflow. Given the limited impacts to the macroinvertebrate communities and the local nature of these impacts, the potential for impact to other species groups including wild birds, fish, and otters is negligible.

*For inspection purposes only.  
Consent of copyright owner required for any other use.*

# 1 Introduction

## 1.1 Project background

The Great Island Combined Cycle Gas Turbine (CCGT) power station is located in the Barrow Estuary, County Wexford, on the south coast of Ireland (Figure 1). It is situated at a point where the estuary splits into two with one branch passing through to Waterford in the west, and the other branch to New Ross in the north. The cooling water from the power station outfall enters the estuary at the shoreline to the east of the site (Figure 1.1). There is a fish pass which discharges abstracted water through the SW8 outfall on the southwest point on the power station where the estuary turns northward. The cooling water intake is in deeper water at the jetty to the south of the site.

**Figure 1.1: Location of the Great Island Combined Cycle Gas Turbine (CCGT) power station**



Source: Google Earth & MML, 2020

Sodium hypochlorite (NaOCl) is used as a biocide in the cooling water system of the power station. An existing Industrial Emissions Directive (IED) licence permits chlorine in the cooling water discharge to a maximum concentration of 0.3 mg/l at the cooling water outfall.

Typical measured chlorine emission values of around 0.2 mg/l at the outfall are compliant with the IED licence. The use of NaOCl has been almost continuous rather than intermittent.

Physical and chemical processes have been investigated using a calibrated three-dimensional (3D) hydrodynamic (HD) model of the Barrow Estuary to simulate the tidal flows and fluvial inputs. The model has been used to simulate the behaviour of the cooling water plume with regards to NaOCl concentrations and pH in the Barrow Estuary. The model accounts for the temperature differences between the cooling water discharge and the receiving water body as well as the temporal and spatial salinity distribution within the estuary. To represent the NaOCl discharge a chlorine tracer has been released in the model at the power station outfall location. Model runs to

simulate the dispersion of the discharge plume and to provide concentrations of NaOCl and water pH both spatially and temporally have been undertaken during neap tidal flow conditions.

In all regards the modelling approach has been conservative to represent as far as practicable potential worst-case scenarios. Model results for NaOCl concentrations and pH have been used to assess the environmental impacts of the cooling water discharge into the Barrow Estuary.

The potential biological effects of the discharge are assessed through a desk-based literature review, subtidal benthic assessment and intertidal survey within the Barrow Estuary, and toxicity analysis of the cooling water discharge Informed by results from numerical modelling of the mixing zone around the cooling water outflow, and the above mentioned desktop review and surveys carried out. this report then considers the most likely environmental impacts of the cooling water discharge on the Barrow Estuary.

## 1.2 Report structure

The report comprises six sections:

- Section 2 – Modelling Approach;
- Section 3 –3D hydrodynamic model setup and includes model calibration and validation results;
- Section 4 – The model calibration and validation results;
- Section 5 – Chlorine dispersion modelling;
- Section 6 – pH dispersion modelling;
- Section 7 – Biological Effects;
- Section 8 – Environmental Impacts; and
- Section 9– Conclusions.

*For inspection purposes only.  
Consent of copyright owner required for any other use.*

## 2 Modelling approach

### 2.1 Introduction

The cooling water discharge from the power station is warmer and thus more buoyant than the ambient estuary water. It will remain in the surface waters of the estuary for some distance from the outfall before becoming entrained and mixed with the estuary waters. Additionally, the fresh river water entering the estuary from locations upstream will mix with the saline estuary water, creating density gradients from north to south as well as vertically. The nature of the density stratification will be dependent upon the freshwater discharge and the estuary salinity. Therefore in order to simulate the behaviour of the cooling water plume in the Barrow Estuary, a three-dimensional (3D) hydrodynamic model (HD) is required to capture accurately these important physical processes.

In the sections below data used in the model build, calibration and validation are described, and the model setup process is explained including: (a) the 3D flexible mesh (FM); (b) model boundary conditions; and (c) model parameterisations. The model calibration and validation processes for spring and neap tides are described, and a range of well-established model performance criteria are used to demonstrate good agreement between model predictions and measurements. Further, sensitivity tests on the simulated power station discharge plume demonstrate good visual agreement with aerial imagery of the plume.

While the natural decrease in NaOCl concentrations in the receiving water due to evaporation and other processes is well-documented, the reported decay rates are variable. To address this uncertainty a conservative approach has been taken whereby the model assumes there is no decrease in NaOCl concentration during a model run.

For inspection purposes only.  
Consent of copyright owner required for any other use.



## 3 Hydrodynamic model setup

### 3.1 Data

#### 3.1.1 Bathymetry

The most up-to-date available bathymetric data from surveys, hydrographic charts and other sources were used to build the model including:

- INFOMAR data – All surveys available for the Barrow Estuary were downloaded from INFOMAR Interactive Web Data Delivery System. The survey available for the Barrow Estuary were the main bathymetric source used to detail the bathymetry of the model. the resolution of the data depended on the survey used, varying from 2m to 5m;
- Emapsite data – Vector data was purchased from emapsite. The data, derived from Electronic navigation Charts, was used to provide additional coverage to the upper Shannon estuary. The data is referred to Chart Datum; and
- EMODnet data (2019) – Freely available data covering the wider offshore area. The data has a resolution of 1/16 arc minutes and it is referred to Mean Sea Level vertical datum.
- All bathymetric data were reviewed, transformed to metres above Ordnance Datum Malin (ODM) and merged using interpolation and smoothing algorithms in a GIS to provide a seamless digital elevation model (DEM).

#### 3.1.2 Water levels

Water level data from Admiralty TotalTide<sup>1</sup> software and the Dunmore East tide gauge was referenced to ODM and used to provide: (a) the boundary conditions to the model; and (b) data for calibration of the model. The location of the water level sites used in the model are shown in **Error! Reference source not found..**

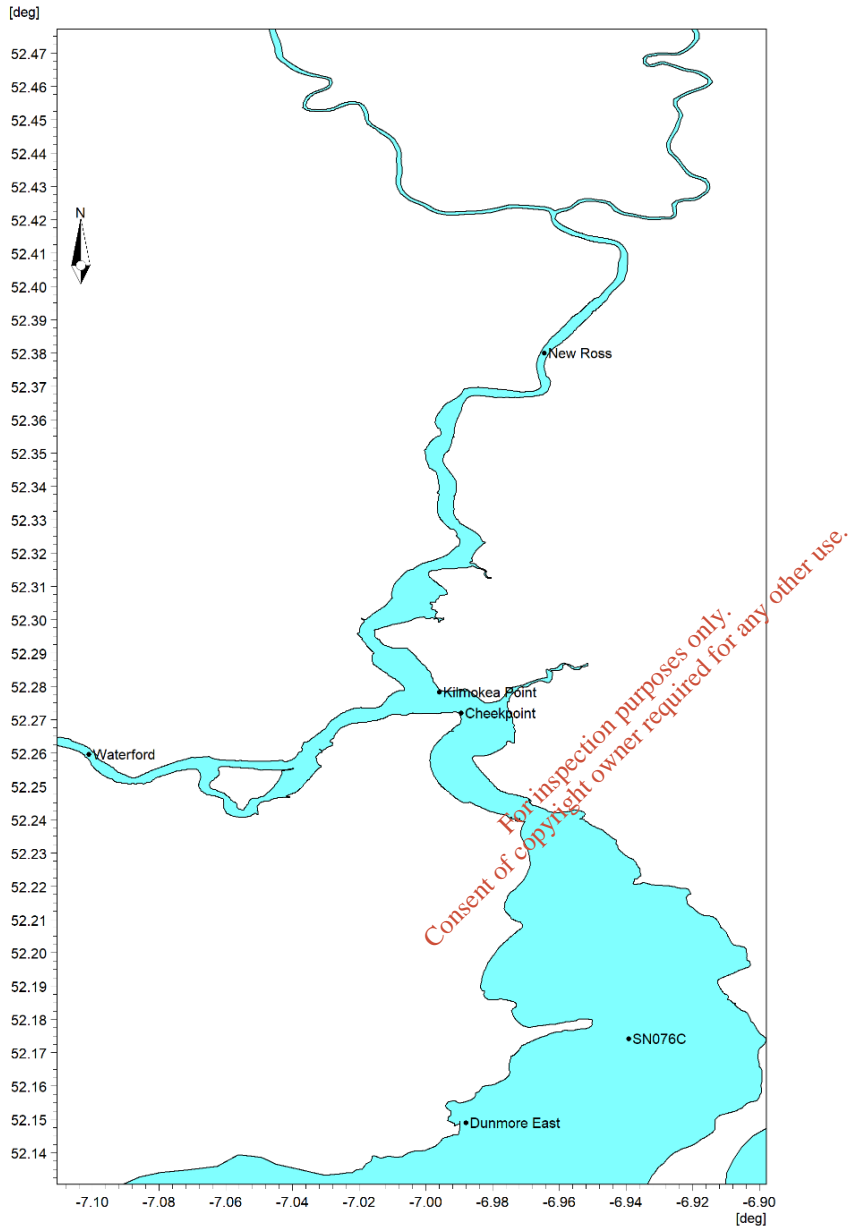
#### 3.1.3 Tidal current speed and direction

Current speed and direction data are required in the model calibration and validation process. Suitable data providing information of the tidal current speed and direction for mean spring and a neap tides were extracted at times coincident with the water level data from TotalTide at the Tidal Diamond location (SN076C) shown in **Error! Reference source not found..**

---

<sup>1</sup> <https://www.admiralty.co.uk/digital-services/admiralty-digital-publications/admiralty-totaltide>

**Figure 3.1: Location of observation water level and current speed data (SN076C tidal diamond)**



Source: MML, 2020

### 3.1.4 Temperature and salinity

Salinity at the model's seaward open boundary has been assumed to be 32 PSU and river water flowing into the model has been assumed to be 0 P.S.U. **Error! Reference source not found..2** shows the salinity measurements at the mouth of the Barrow Estuary (EPA site SR660) where it meets with the Atlantic Ocean. On average there are approximately three times per year when single salinity measurements (surface and bed) have been recorded at this site. What is evident when comparing the salinity against the river flow rates, is that on the occasions where the

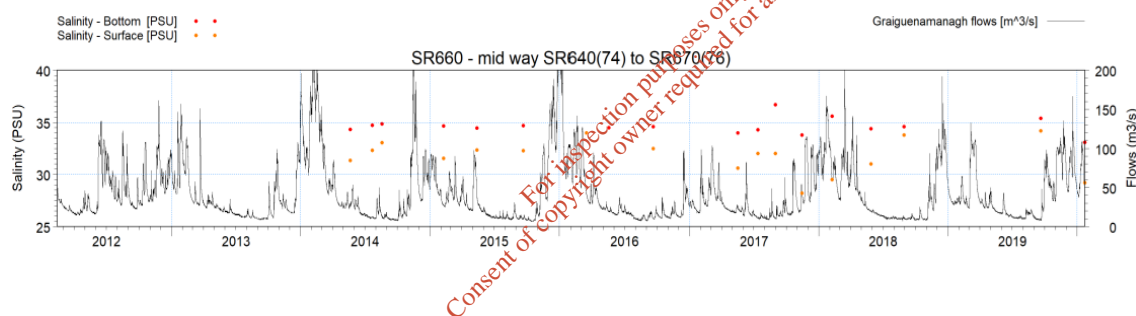
measurement coincides with high river flow, the surface salinity drops. This is not unexpected as the more buoyant freshwater will be more evident. The model simulation presented in this report coincides with a period where there were no salinity measurements available.

Looking at the near-bed measurements the salinity ranges from 34-36 PSU at this estuary mouth location, whereas the surface measurements range from 28-34 PSU. Given this range of salinity a mid-value of 32 PSU has been applied to the model boundary throughout its depth. Given the range of measurement values and a lack of a time-series of salinity measurements outside of the estuary mouth, based on our experience a value of 32 PSU is a reasonable assumption, especially given that during the winter time there may be increased vertical mixing due to waves as well as relatively high river flow.

Ambient estuarine water temperature in the model has been assumed to be 9°C, a typical value for January/February. While this may appear to be arbitrary, it makes no difference to the model setup since this assumes that the cooling water discharge is always 10°C<sup>2</sup> above the ambient temperature. This excess temperature provides buoyancy to the cooling water required to represent plume buoyancy.

River flow rates into the model were taken from the Office of Public Works<sup>3</sup> (OPW) and applied as a time-series of flow rate at the three main tributaries. The river discharges were applied in the surface layer of the model with a temperature of 9°C and a salinity of 0 P.S.U.

**Figure 3.2: EPA salinity measurements (surface and bed) compared against upstream river flow at Graiguenamanagh**



## 3.2 Model setup

### 3.2.1 Horizontal and vertical references

The model was set up using the Geographic Coordinate System, (Lat/Long), based on the WGS84 horizontal datum. The vertical reference datum for the model bathymetry and boundary conditions is referred to metres above Ordnance Datum Malin (mOD Malin). It is noted that Ordnance Datum Malin is the same as Ordnance Datum Belfast and Ordnance Datum Dublin (also called Poolbeg datum) is 2.7m below Ordnance Datum Belfast.

### 3.2.2 Model mesh and extent

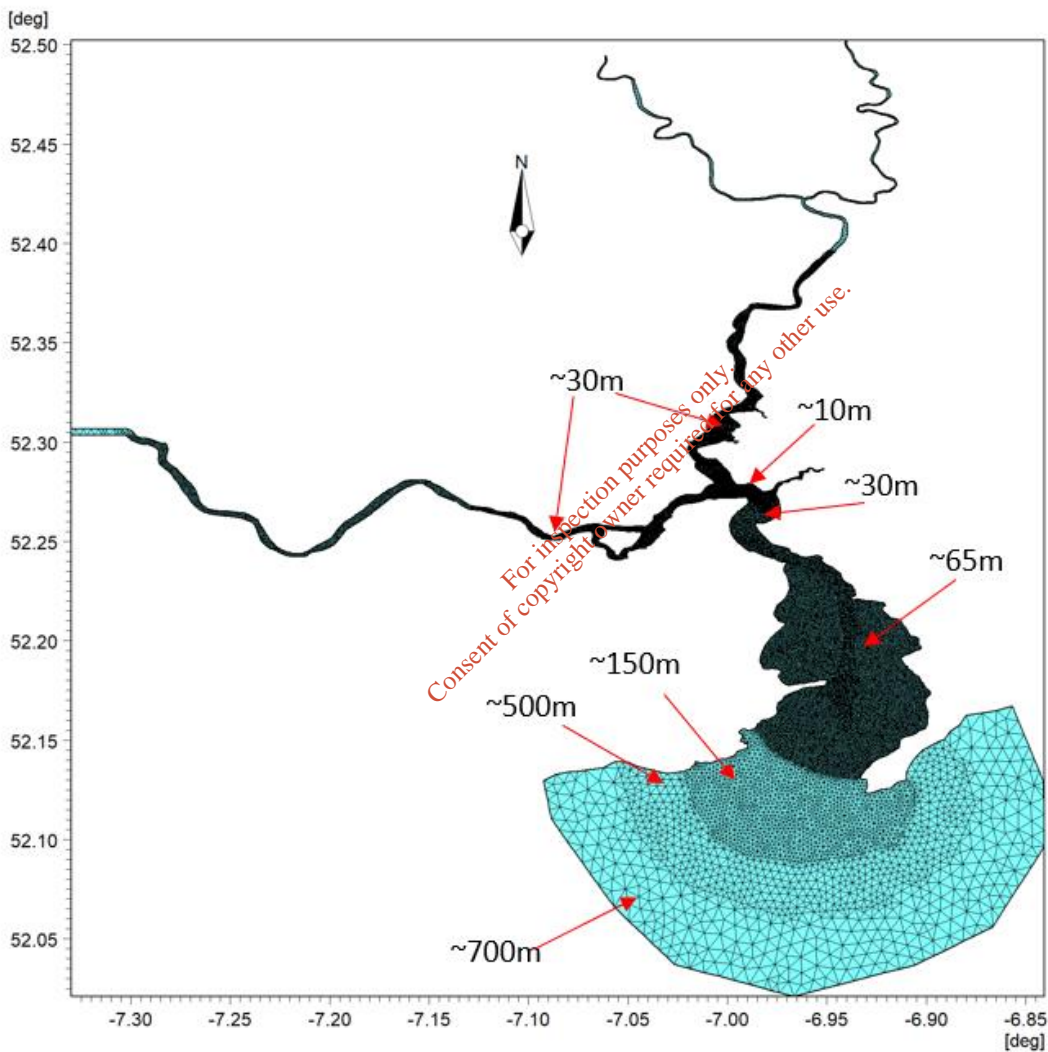
To ensure that the tidal flows were represented correctly in the Barrow Estuary, the model's offshore boundary was defined in the offshore area of the estuary, approximately 11km from the estuary mouth. The MIKE3 HD flexible mesh (FM) comprises triangular elements used to simulate

<sup>2</sup> Measurements of intake and outfall temperature were made available by SSE. The 10°C excess temperature was the greatest value recorded.

<sup>3</sup> [http://waterlevel.ie/hydro-data/search.html?rbd=SOUTH\\_EASTERN\\_RBD](http://waterlevel.ie/hydro-data/search.html?rbd=SOUTH_EASTERN_RBD)

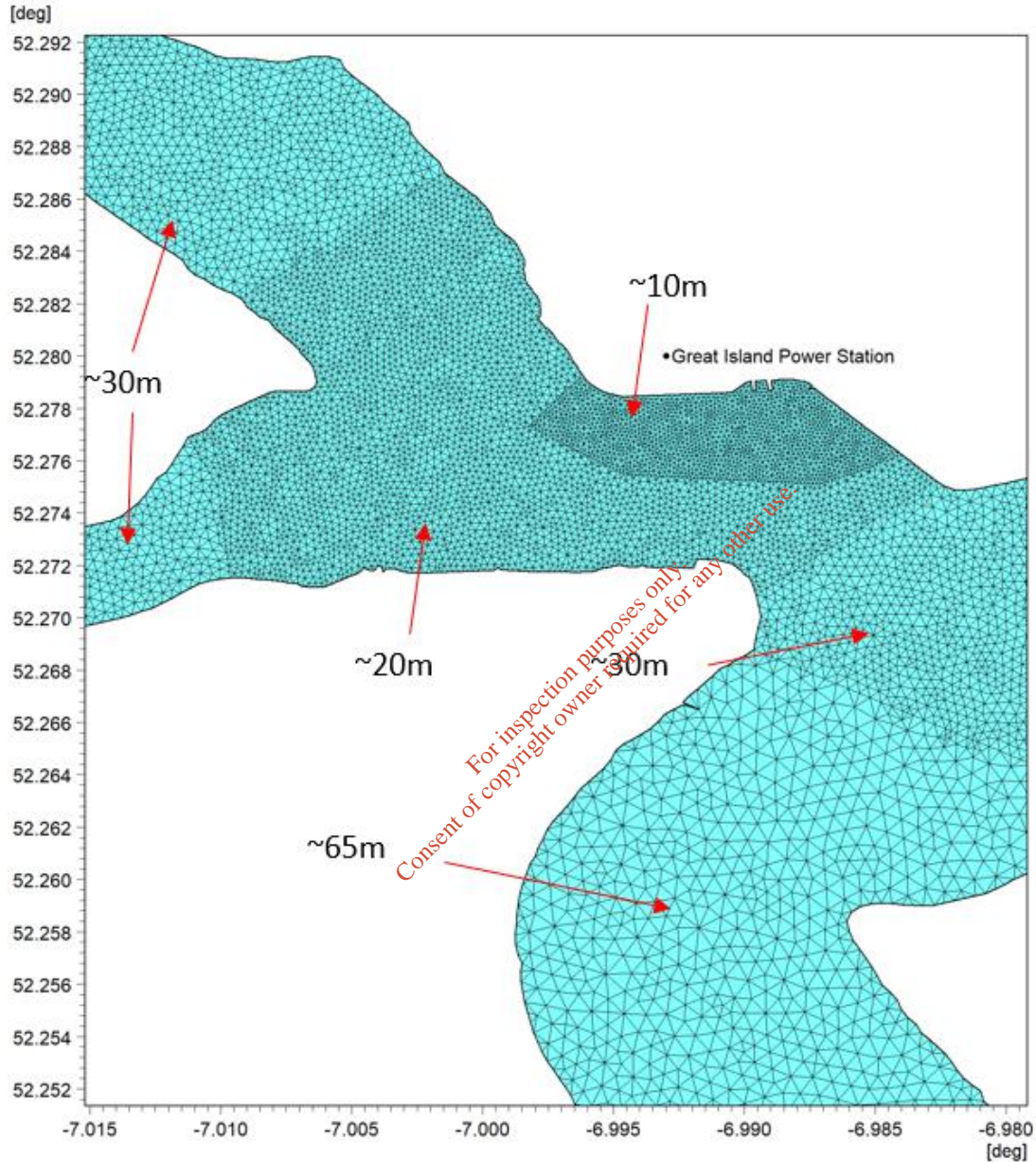
the movement of water under the influence of tides and the effect of density variations. The resolution of the model mesh is coarser in the offshore region, with elements of approximately 600m. The mesh resolution in the estuary was variable with side lengths of 70 to 80m, 9 to 12m and 30 to 40m in the outer part of the estuary, the vicinity of the project site and the intertidal channels, respectively. **Error! Reference source not found.** shows the model mesh for the entire model domain and **Error! Reference source not found.** 3.4 shows an enlarged view around the Great Island Power station.

**Figure 3.3: MIKE3 FM HD overall model mesh and approximate mesh resolution**



Source: MML, 2020

**Figure 3.4: MIKE3 FM HD model mesh in the vicinity of the Great Island Power Station and approximate mesh resolution**



Source: MML, 2020

### 3.2.3 Vertical mesh

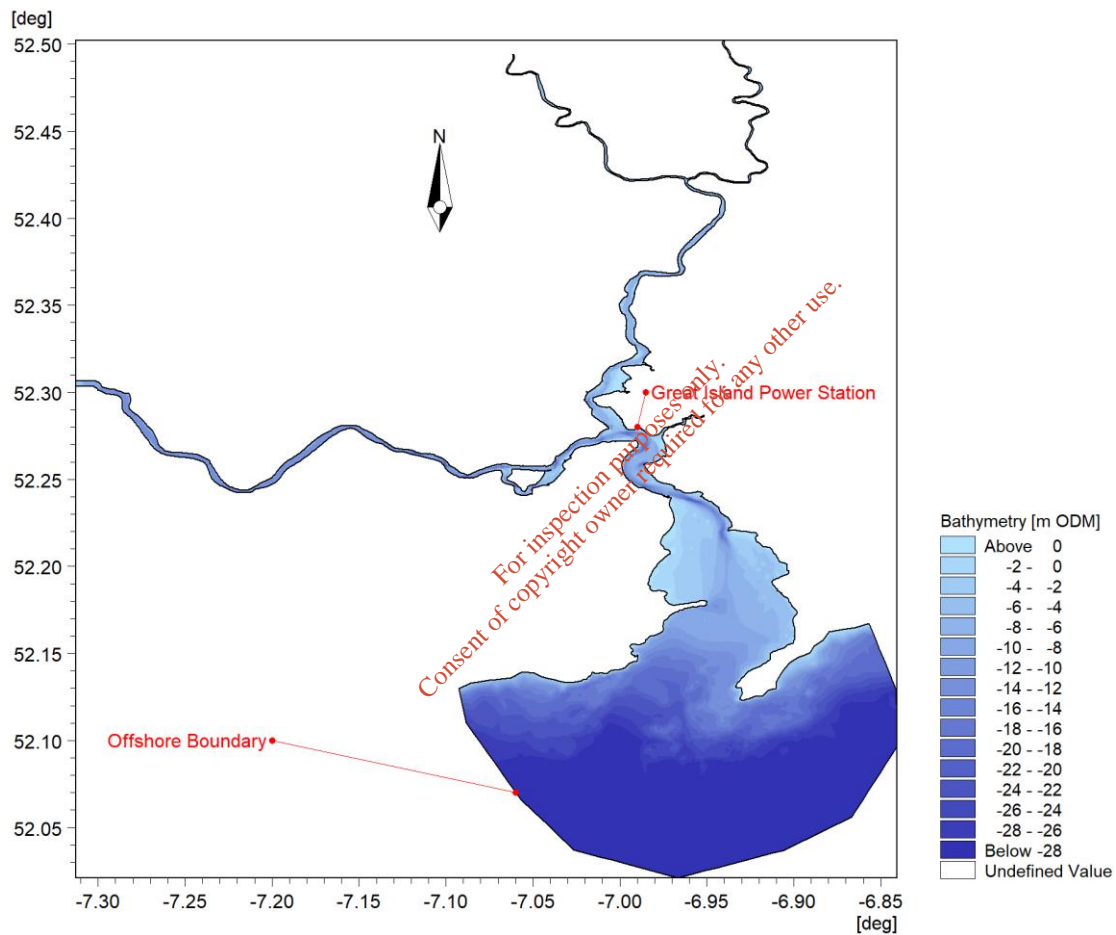
To represent the water column structure the 3D vertical mesh structure is divided using 10 vertical *sigma* layers. The layer number is selected from the lowest active layer increasing upwards, towards the surface, being layer 1 close to the bed, while layer 10 is at the water surface. It is noted that in a sigma layer mesh, the number of active layers in the water column is always be

the same in any point in the domain irrespective of the water depth. In the present study each layer had a thickness defined as being 10% of the overall water depth across the model domain.

### 3.2.4 Model bathymetry

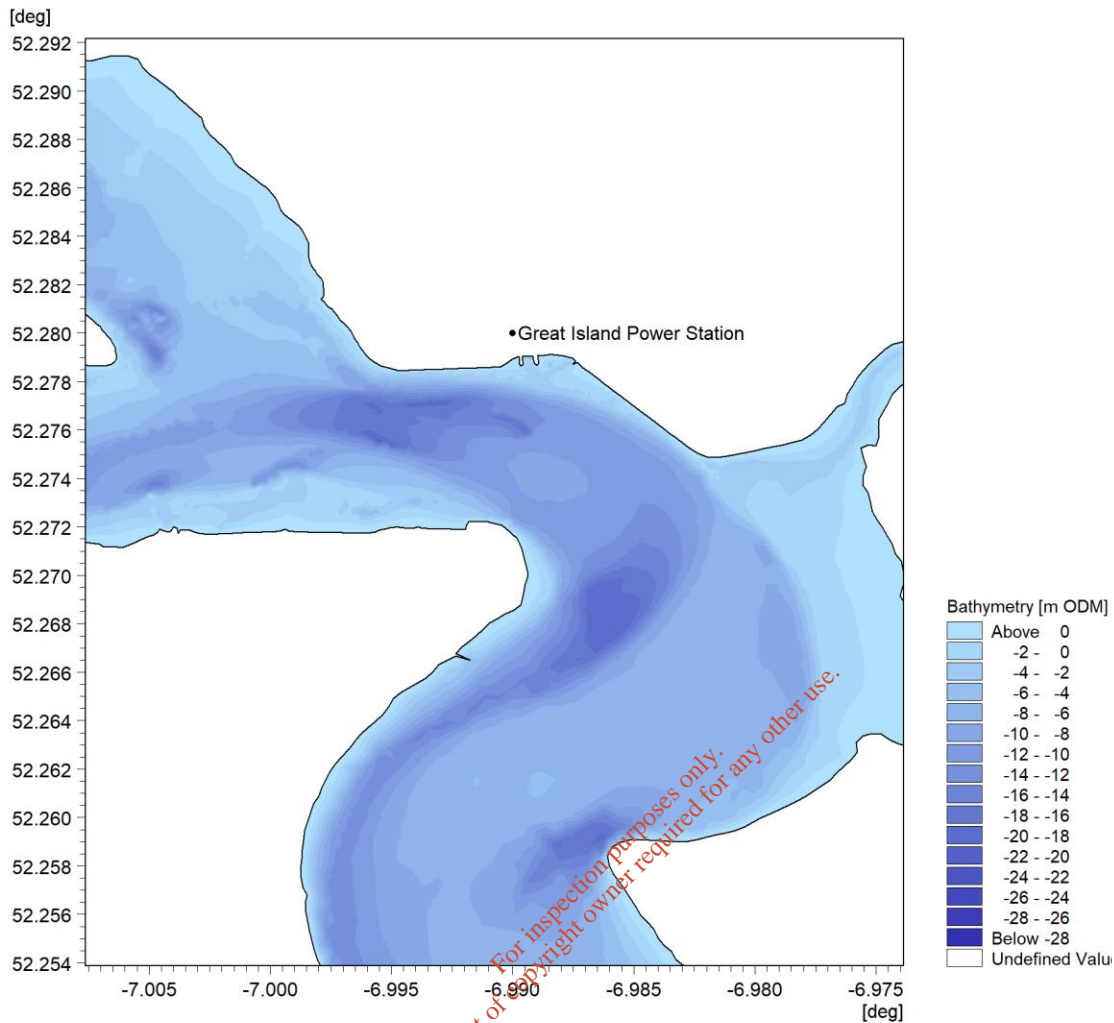
The bathymetric data (Section 3.1.1) was then interpolated onto the model mesh to define the bathymetry in the model domain. The overall model domain and the interpolated bathymetry can be seen in Figure 3.5, with an enlarged view around the project site shown in Figure 3.6.

**Figure 3.5: MIKE3 FM HD model bathymetry of entire domain**



Source: MML, 2020

**Figure 3.6: Model bathymetry in the vicinity of the project site**



Source: MML, 2020

### 3.2.5 Boundary conditions

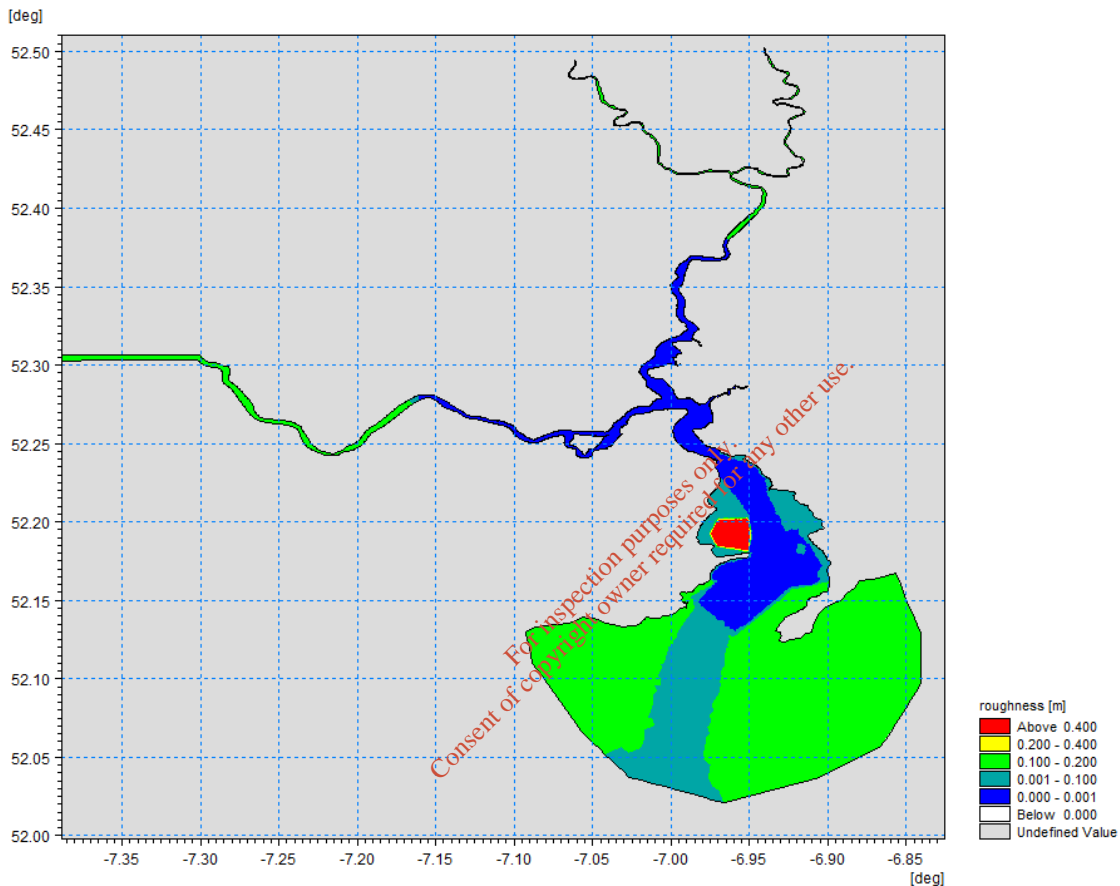
After several tests to determine the most appropriate offshore open boundary conditions (location shown in **Error! Reference source not found.**) the tidal data from Dunmore East was selected and applied around the entire open boundary. To compensate for the time-delay for the tidal wave travelling to Dunmore East just inside the estuary mouth, a time-shift of 7 minutes was applied. This slight adjustment enabled a very good reproduction of the tide at Dunmore East propagating into the estuary.

### 3.2.6 Bed roughness

Bed roughness provides frictional resistance to the flow of water and is used as a calibration parameter in the model to obtain the best possible agreement between measured and predicted current speeds and water levels within the estuary. Sensitivity tests were undertaken to obtain the optimal bed roughness across the model domain (Figure 3.7) giving values of 0.001m or lower in the main body of the estuary and higher roughness values of 0.1m in the intertidal areas where bed features are present. The exception to this was over the western mudflat shell fisheries where the roughness was increased to 0.2m to reflect known bed disturbances.

Offshore roughness values varied between 0.1m in the estuary channel to 0.2m elsewhere to represent ripples and other bed features likely to be present given the strength of the tidal flows, wave action and the nature of the bed sediments. Upstream, in the tributaries, the roughness was defined in the calibration process as being 0.001m in the lower reaches and increasing in magnitude further upstream.

**Figure 3.7: Bed roughness length as used in the model**



Source: MML, 2020

### 3.2.7 Eddy viscosity

Following established 3D modelling protocols, the horizontal eddy viscosity was selected with a constant Smagorinsky formulation coefficient of 0.25 (Smagorinsky, 1963). This is within the range recommended by DHI. The vertical eddy viscosity was by the *k-epsilon*<sup>4</sup> formulation using the default parameters in the model.

### 3.2.8 Dispersion

Whilst the horizontal and vertical eddy viscosity provides a means to represent sub-grid scale turbulence in the hydrodynamic model, the temperature and salinity module uses an

<sup>4</sup> The k-epsilon ( $k-\epsilon$ ) turbulence model is the most common model used in Computational Fluid Dynamics (CFD) to simulate mean flow characteristics for turbulent flow conditions.



advection/dispersion model to move and disperse the temperature and salinity. In the present model the vertical dispersion has been taken as a scale with a scaling factor of 0.1 to represent the vertical eddy viscosity. In our experience finite volume models such as MIKE3 FM HD have significant numerical dispersion brought about by the numerical method used to solve the dispersion equations and thus to be conservative the horizontal dispersion in the present model was turned off. The simulated Chlorine and pH components in the model (Sections 5 and 6), also used the same horizontal and vertical dispersion parameters as the temperature and salinity.

As a check on the assumptions made regarding model dispersion settings, the modelled plume behaviour was compared visually with aerial imagery. With the horizontal dispersion turned off, the model plume was very similar in spatial extent to the aerial image, especially in the lateral direction where dispersion is most obvious.

### 3.2.9 River flows

The freshwater input of the rivers was included into the model as discharge sources, with a salinity of 0 PSU and discharging into the upper vertical layer. The river flow data was used for the calibration period as there were no extreme events during this period.

*For inspection purposes only.  
Consent of copyright owner required for any other use.*

## 4 Hydrodynamic model calibration and validation

### 4.1 Hydrodynamic Model Calibration

To ensure the cooling water discharge plume behaviour is correctly represented it is important that the water level and current speed predictions made by the MIKE3 FM HD model compare well with measured data. The level of agreement between predicted and observed values is optimised through the model calibration and validation process.

Noting the constraints imposed by the specific model application and data limitations, the process of model calibration involves varying model parameters, boundary conditions, bathymetry, bed roughness etc. to reproduce as accurately as possible measured data at key locations within the model domain. Without changing the model parameters/setup derived during the calibration, the model is then validated to establish that model can predict with the required accuracy the hydrodynamic processes from a different period and/or location. This approach is widely accepted as demonstrating that the model is robust enough to be applied in subsequent simulations of different periods or input conditions.

### 4.2 Performance Criteria

The evaluation of whether an established model provides a sufficiently accurate description of the environment depends in general on the specific objective for the individual model. Traditionally, the evaluation of performance has been based on visual comparisons (e.g. by time-series plots or instantaneous plan/transect plots of modelling results and monitoring data). More recently, a quantitative approach for the performance control has been introduced, where the general discrepancy (or match) between model and monitoring data is expressed numerically.

Simple statistics that demonstrate the level of agreement between measured/observed data and model prediction at a chosen location in the model domain include the mean and peak differences (often expressed as a percentage) and the standard deviation. A number of quality indices can be used to demonstrate the statistical agreement between model predictions and observations such as root mean square error (RMSE), bias and correlation coefficient of determination ( $R^2$ ):

- Root Mean Square Error (RMSE) - RMSE is a measure of the residuals between the model prediction and measured observation. Smaller value indicates better agreement;
- Bias - Bias expresses the difference between an estimator's expectations and the true value of the parameter being estimated and can be defined as being equal to the mean error statistics in the data;
- Pearson product-moment coefficient ( $R$ ) – The  $R^2$  measures the best linear fit between observed and simulated values. It ranges from 0 to 1 with larger values indicating a better fit. Please note that the measure is insensitive to bias and proportionality, and hence large  $R^2$  values may be obtained for models that have serious errors. Another drawback of the  $R^2$  measure is that it is more sensitive to outliers than values close to the mean.

Model performance metrics defined by Williams & Esteves (2017), have been used to assess the calibration and validation performance of the hydrodynamic model. Table 4.1 summarises the guidelines against which the calibration and validation of the Great Island model have been assessed measured.

**Table 4.1: Statistical guidelines to establish calibration standards for a minimum level of performance for coastal and estuarine hydrodynamic models**

Predictions		RMSE	Bias
Water level (coast)	± 10% of the measured level.	< 0.10	> 0
Water level (estuary)	± 10% (mouth); ± 25% (head) of the measured level.	< 0.20	> 0
Water level phase (coast)	± 15% of the measured phase.	< 0.20	> 0
Water level phase (estuary)	± 15% (mouth); ± 25% (head) of the measured phase.	< 0.25	> 0
Average current speed	± 10% to 20% of the measured speed.	< 0.10	> 0
Peak current speed	Within <0.05m/s (very good), <0.1m/s (good); <0.2m/s (moderate) & < 0.3m/s (poor) of the measured peak speed.	< 0.15	> 0
Current direction (coastal)	± 10° of the measured direction.	< 0.25	> 0
Current direction (estuary)	± 15° of the measured direction.	< 0.30	> 0

Source: Williams & Esteves (2017).

### 4.3 Calibration results

The MIKE3 FM HD model was run with average river flows for a period of 4 days 4 hours (8 tides) between 21/1/2019 05:30 UTM and 25/1/2019 09:30 UTM. The location of the water level data used for comparisons with the model results is shown in Figure 3.1

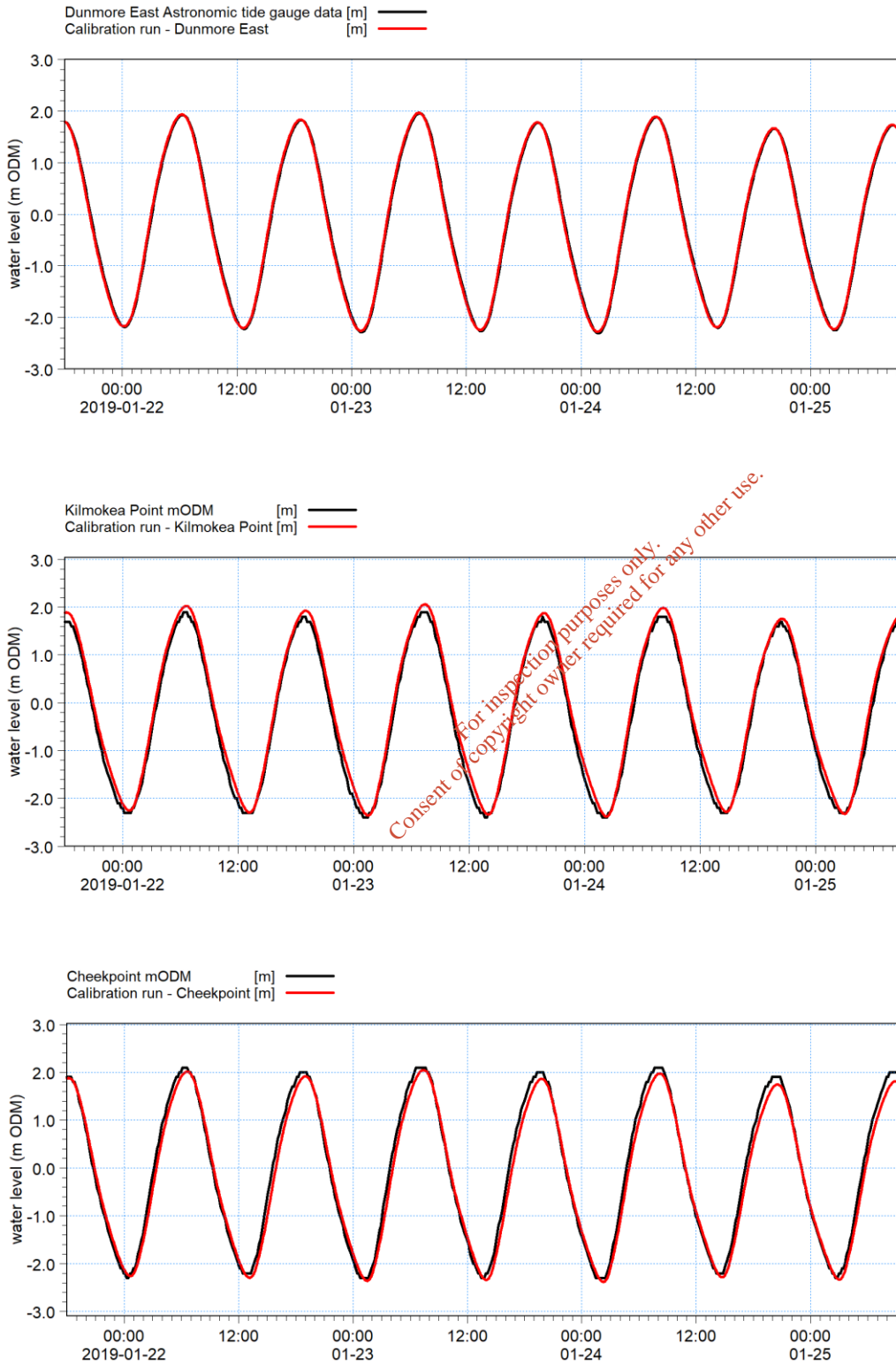
The outfall/intake was included in the model, as was the temperature and salinity variation in the model, and for efficiency calibration was undertaken initially using 3 vertical layers. This was increased to 10 vertical layers for the main simulations. It is noted that the reduced number of layers did not make any significant difference to the water levels or current speed in the model at the calibration locations. However, for the main simulations post-calibration, the increase to 10 vertical layers was included to correctly resolve the vertical structure of the buoyant plume.

#### 4.3.1 Water level

Figure 4.1 and Figure 4.2 show comparisons between the water level data and the calibrated model results at the locations shown in Figure 3.1. In general, the water levels simulated by the model are able to reproduce the observed tide gauge data at Dunmore East, and the TotalTide data at Cheekpoint and Kilmokea Point, very well.

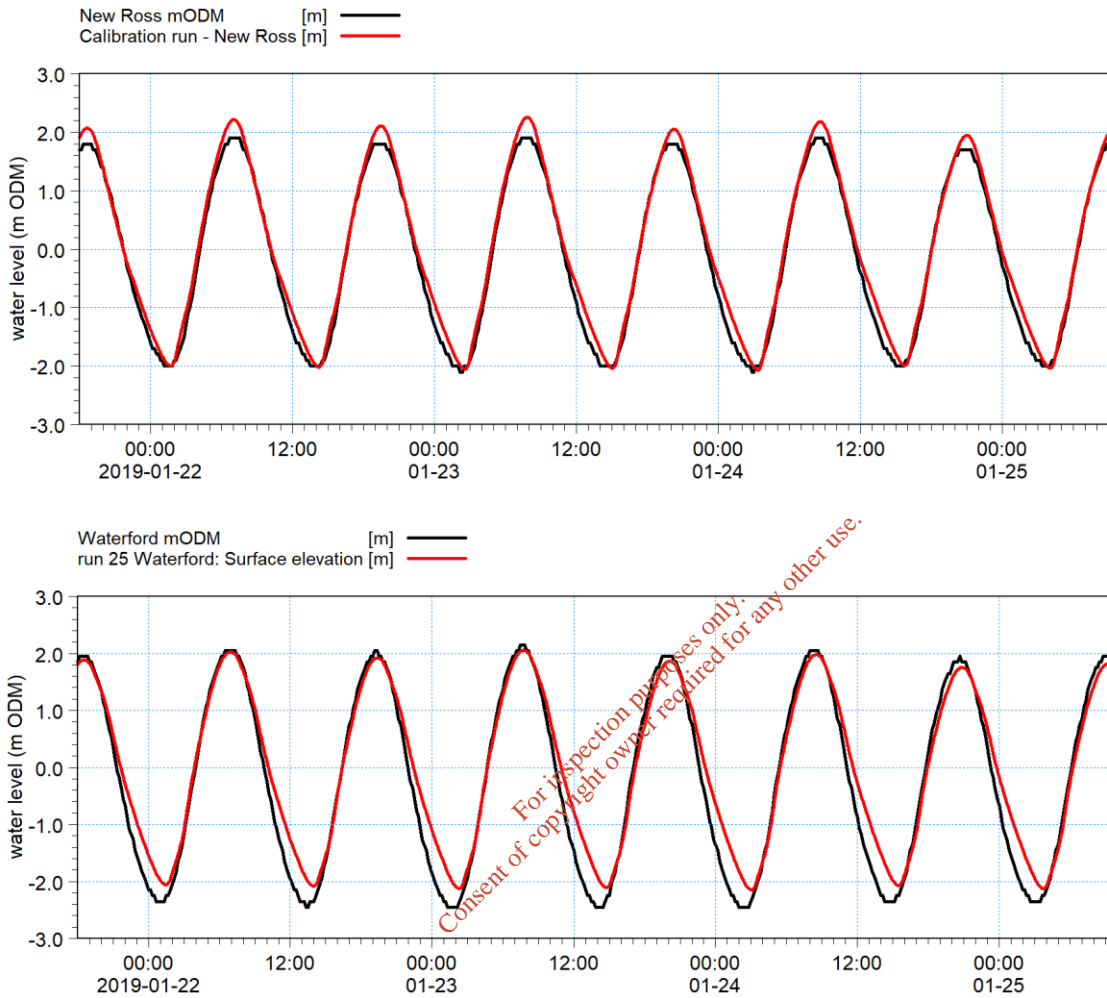
At New Ross the model slightly over-predicts high-water levels and water levels during the latter part of the ebb tide. This is attributed to a lack of bathymetric data for this region of the model where data have been interpolated or inferred. Likewise, at Waterford there was no bathymetric data available upstream. Water levels at high water are reproduced well, although the late ebb tide and low water are over-predicted. Although for the reasons previously stated the bathymetry in these upper reaches is not accurate, the predicted water level results are considered to be reasonable and have allowed the tidal volume for the upper reaches of the estuary to be incorporated further downstream in the main body of the estuary, as well as allowing the tidal wave to propagate upstream at the right rate.

**Figure 4.1: Spring tide comparisons between observed (black) and simulated (red) water levels**



Source: MML, 2020

**Figure 4.2: Spring tide comparisons between observed (black) and simulated (red) water levels**



Source: MML, 2020

Error statistics for water levels shown in Table 4.2 show that the root mean squared error (RMSE) compared with the tidal range is less than 10% at all five locations. As would be expected the RMSE is lower at Dunmore East (closer to the estuary mouth), than the other locations further upstream. For all locations the bias is less than 0.2m and the  $R^2$  value is greater than 0.95. Therefore, these statistics combined with the visual comparisons shown in Figure 4.1 and Figure 4.2 have led us to conclude that the model is suitably well calibrated for water levels for the purpose of this study.

**Table 4.2: Spring tide error statistics for water levels**

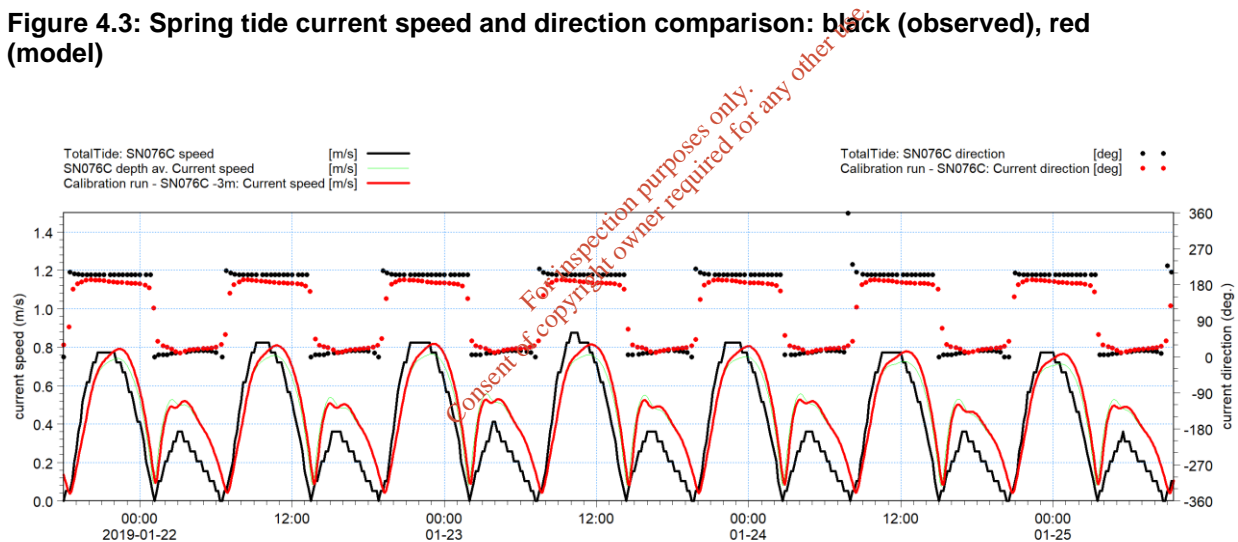
	Dunmore East	Cheekpoint	Kilmokea Point	Waterford	New Ross
Mean Error (m) (Bias)	-0.002	0.09	-0.14	-0.18	-0.15
Root Mean Square Error (m) (RMSE)	0.08	0.11	0.16	0.37	0.19
Correlation, R <sup>2</sup>	0.999	0.999	0.997	0.985	0.995
RMS error/tidal range (%)	2.1%	2.8%	4.1%	8.6%	4.9%

Source: MML, 2020

### 4.3.2 Tidal current speed and direction

A comparison between the model speed and direction and the tidal diamond data (SN076C in Figure 3.1) is shown in Figure 4.3. In this figure the predicted current speeds at 3m below the surface are shown in red and represent as close as possible the vertical location in the water column of measured data from the tidal diamond (i.e. the typical draft of a boat). The predicted depth-averaged current speed is also shown in green.

**Figure 4.3: Spring tide current speed and direction comparison: black (observed), red (model)**



Source: MML, 2020

In general, comparison between model predictions and measured tidal current speeds is good. However, there are a few features where the comparisons are less favourable:

- The magnitude of current speeds on the ebb tides are greater than those on the flood. Capturing this asymmetry is important as this partly determines the overall transport direction of the discharge plume over longer timescales;
- Although the magnitude of the peak speeds matches very closely, the peak ebb tide velocity lags the observed tidal diamond data; and
- During the flood tide the peak speeds are over-predicted in the model by approximately 0.1 to 0.15m/s.

Although many model tests were undertaken to try and improve the representation of tidal currents in the model, none were especially successful. It is considered that remaining differences between predicted and measured tidal flows could be attributable to: (a) high river flows at the time of the measurements that influenced the flood current speeds directly; and/or (b) the bathymetry at the time of the measurements was different to the more up-to-date bathymetry used in the model (e.g. the present day channel has been dredged).

## 4.4 Model validation

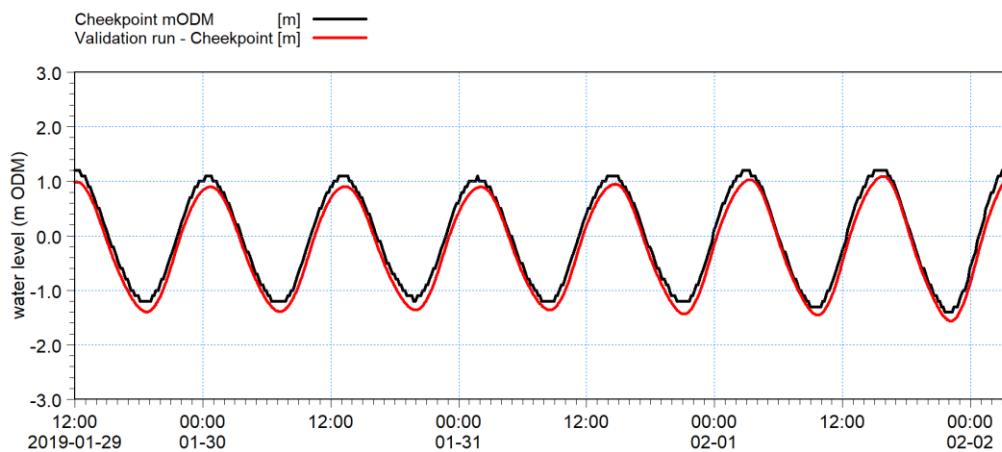
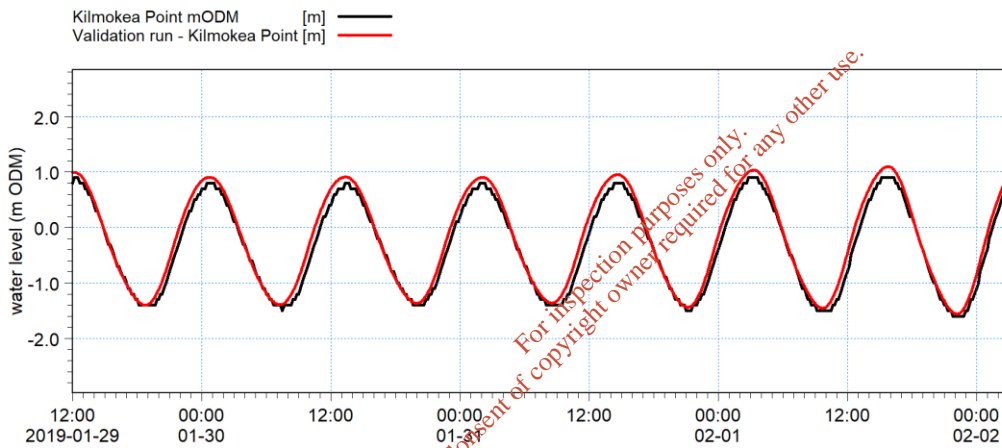
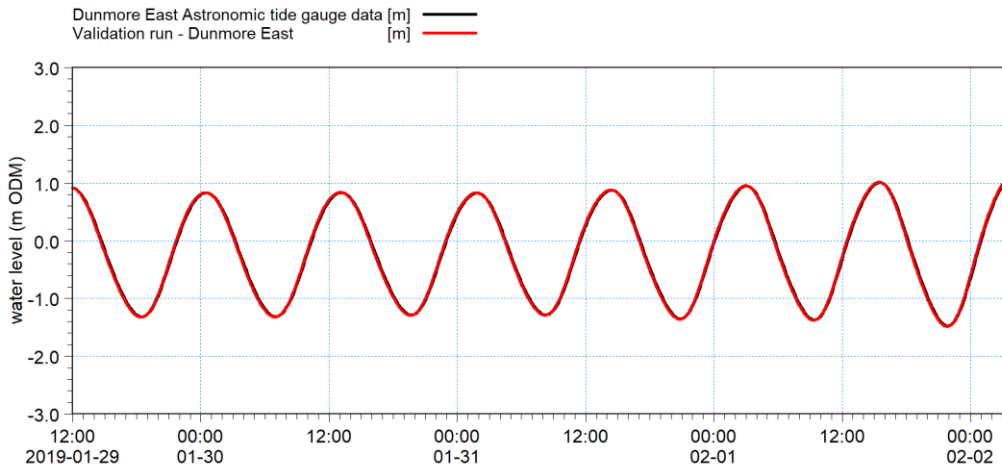
For the validation of the model, the model parameters obtained during the calibration phase are used for comparison against a different dataset or range of tides. In this instance the model has been run for a series of neap tides to determine how well the model can reproduce the hydrodynamic conditions without any changes to the model parameters.

### 4.4.1 Water level

The hydrodynamic model was run for a period of 4 days 4 hours (8 tides) during the period 28/1/2019 23:30 through to 02/02/2019 03:30. The location of the water level data used for comparisons with the model results is shown in Figure 3.1. The outfall/intake was included in the model, as was the temperature and salinity variation in the model, and for efficiency validation was undertaken initially using 3 vertical layers. This was increased to 10 vertical layers for the main simulations. It is noted that the reduced number of layers did not make any significant difference to the water levels or current speed in the model at the validation locations. However, for the main simulations post-validation, the increase to 10 vertical layers was included to correctly resolve the vertical structure of the buoyant plume.

Figure 4.4 and Figure 4.5 show a comparisons between the water level data and the validated model results at the locations shown in Figure 3.1. In general, the water levels simulated by the model reproduce very well the observed tide gauge data at Dunmore East, and the TotalTide data at Cheekpoint and Kilmokea Point. However, it is noted that there appears to be a vertical shift in the Cheekpoint model relative to the TotalTide data. It is not known the cause of this, although the model boundary is the same as for the spring tide, this might suggest that there are some small variations in the mean water level in the TotalTide data. The differences are small however and are considered not to affect the results of the dispersion modelling. At New Ross and Waterford water levels are reproduced well and in fact better than during the spring tides although high water levels at Waterford are under-predicted by about 0.1 to 0.2cm.

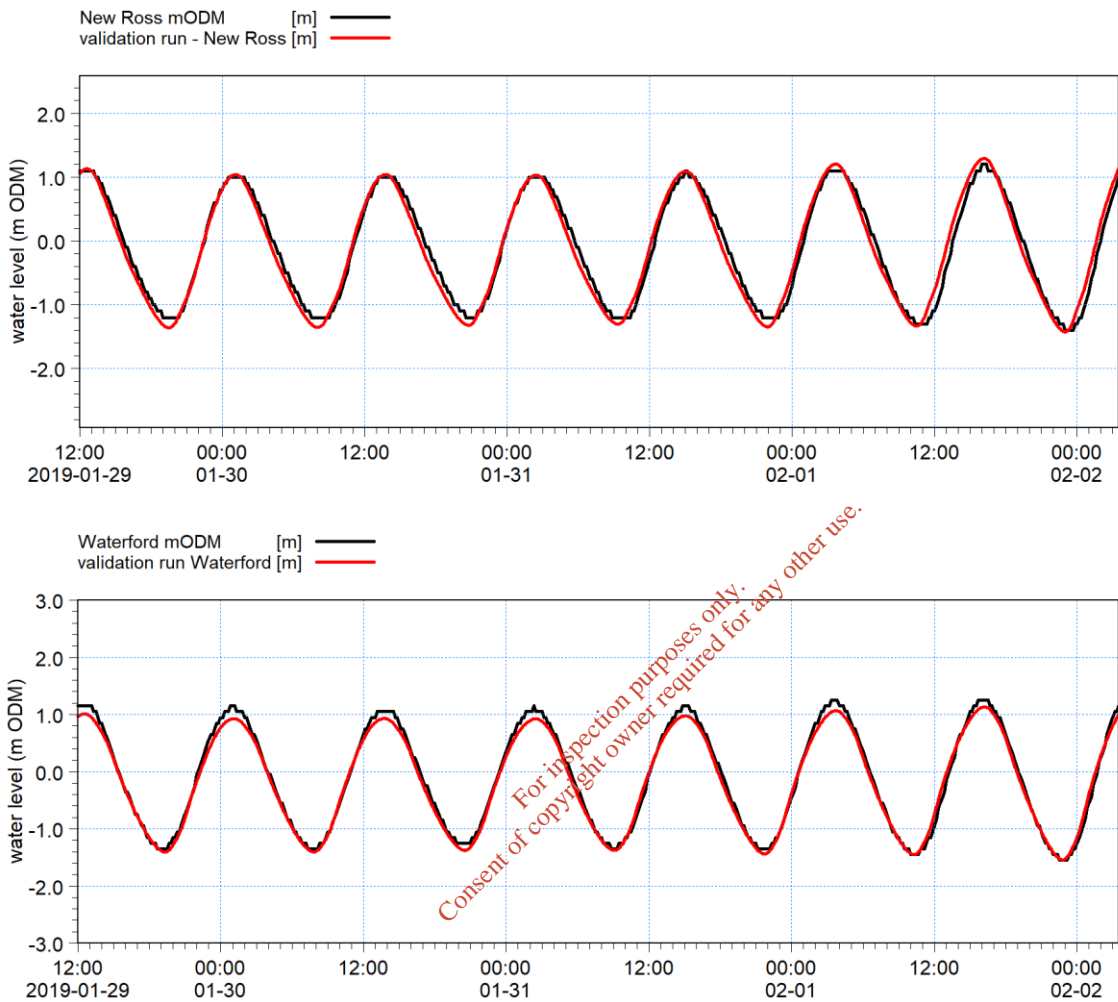
**Figure 4.4: Neap tide comparisons between observed (black) and simulated (red) water levels**



Source: MML, 2020



**Figure 4.5: Neap tide comparisons between observed (black) and simulated (red) water levels**



Source: MML, 2020

Model validation performance statistics for the neap tide period are shown in Table 4.3. This table shows that the root mean squared error (RMSE) compared with the tidal range is less than 10% at all five locations. As would be expected the RMSE is lower at Dunmore East (closer to the estuary mouth), than the other locations further upstream. For all locations the bias is less than 0.2m and the  $R^2$  value is greater than 0.95. Therefore, these statistics combined with the visual comparisons shown in Figure 4.4 and Figure 4.5 have led us to conclude that the model has been successfully validated for water levels during the neap tide period.

**Table 4.3: Neap tide model validation performance statistics for water levels**

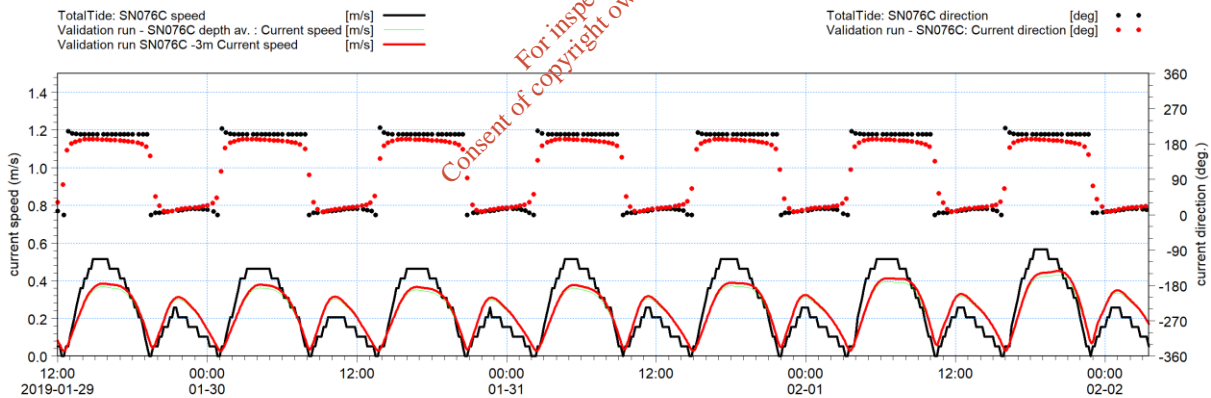
	Dunmore East	Cheekpoint	Kilmokea Point	Waterford	New Ross
Mean Error (m)	-0.01	0.17	-0.12	0.06	0.02
Root Mean Square Error (m)	0.08	0.18	0.15	0.10	0.14
Correlation	0.997	0.989	0.991	0.997	0.993
RMS error/tidal range (%)	2.4%	4.5%	3.8%	2.3%	3.8%

Source: MML, 2020

#### 4.4.2 Tidal currents

A comparison between the model speeds/directions and the tidal diamond data (location SN076C shown in Figure 3.1), is shown in Figure 4.6. In general, the comparison is good, with the current speeds during the neap tide flood period showing a better comparison than the flood period during the spring tides. The ebb tide currents appear to have a better phase representation than the spring tides, although peak speeds are under-predicted by about 0.1-0.15m/s. It should be borne in mind the nature of the Tidal Diamond data and the limitations/assumptions inherent in their use (see above). However, the lower peak current speeds predicted by the model will result less advection of the power station discharge plume during the time of peak ebb flow and thus the model is conservative.

**Figure 4.6: Neap tide current speed and direction model validation comparison: black (observed), red (model)**



Source: MML, 2020

Table 4.4 shows the model performance statistics for the spring (calibration) and neap (validation) current speeds. Whilst not perfect, the calibration is considered reasonable given the uncertainties in the tidal diamond data. Table 4.4 also shows that the model performance statistics for the neap tide are better than for the flood. Since for conservatism the simulations of the discharge plume dispersion have been undertaken during neap tides, when NaOCl concentrations are likely to reach their highest values in the immediate estuarine environment, the better model performance for ebb tides is judged to demonstrate an acceptable model calibration for the purposes of the present study.

**Table 4.4: Spring and neap tide error statistics for current speeds**

	SN076C - spring tides (model calibration)	SN076C - neap tides (model validation)
Mean error (m/s)	-0.09	-0.004
Root Mean Square Error (m/s)	0.16	0.08
Correlation R <sup>2</sup> (-)	0.898	0.909

Source: MML, 2020

To summarise, the model has been calibrated and validated for water levels at several locations, and current speeds at one location in the main estuary channel. Visual interpretation and statistical analysis have shown the model to be suitable for the intended purpose of simulating the behaviour of the cooling water plume and associated NaOCl in the estuary.

For inspection purposes only.  
Consent of copyright owner required for any other use.

## 5 Chlorine dispersion modelling

### 5.1 Introduction

The sodium hypochlorite (NaOCl) biocide used in the treatment of biological fouling within the Great Island power station cooling system is mixed with the cooling water and is subsequently discharged into the estuary where it mixes and disperses. In the NaOCl dispersion modelling reported here (hereafter referred to as *chlorine modelling*) the discharge from the power station has been included in the calibrated and validated MIKE3 FM HD model as a tracer and the simulated flow field from the hydrodynamic model is used to transport and disperse the water plume and define its temporal and spatial characteristics. The results from plume simulations have then been used to assess the potential impacts on the estuary.

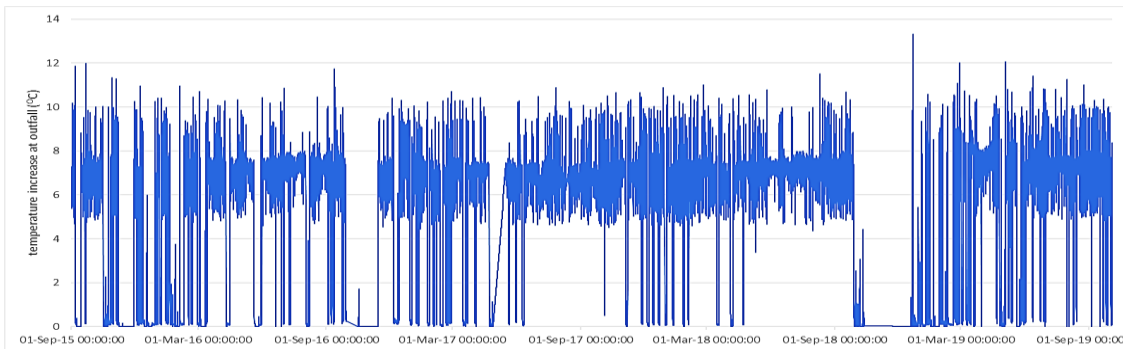
### 5.2 Boundary and outfall configuration in the model

To simulate tidal variations in water level and currents throughout the estuary the MIKE3 FM HD model was run for eight neap tides. The use of neap tides represents a conservative approach likely to result in higher chlorine concentrations than springs due to the reduced mixing and distance travelled over the flood or ebb period of the tide. The model was run as previously described with ten, equally spaced, vertical layers to capture the buoyancy of the warmer outfall plume and density gradient attributable to salinity differences across the model domain.

Temperature at the outfall was assumed in the model to be 10°C higher than the ambient estuary water temperature of the water was assumed to be 9°C (sea temperature for January/February). River temperatures were also assumed to be the same ambient temperature as the sea water. The model allows for potential cooling water recirculation effects to be included in the simulations. The excess temperature selected was based on the data provided by SSE at the intake and outfall captured over several years (Figure 5.1). Whilst there are some isolated higher temperature increases, the mean temperature increase appears to be closer to +7°C to +8°C, with a generally higher plateau at about +10°C. This higher temperature would produce more buoyant outfall discharge and hence keep the plume closer to the surface for longer, thus reducing the vertical mixing and therefore producing higher surface concentrations of the chlorine tracer. It is therefore considered to be a conservative approach.

Salinity of the river water was assumed to be 0 PSU (practical salinity units), whilst that of the water entering the model's offshore boundary was set at 32 PSU. Initial conditions in the model also had a salinity of 32 PSU. It was found that the river water mixed vertically with the estuarine water by the time it had reached the intake / outfall locations and therefore salinity was less important for the outfall discharge buoyancy than the increase in temperature.

**Figure 5.1: Temperature increase from intake to outfall**



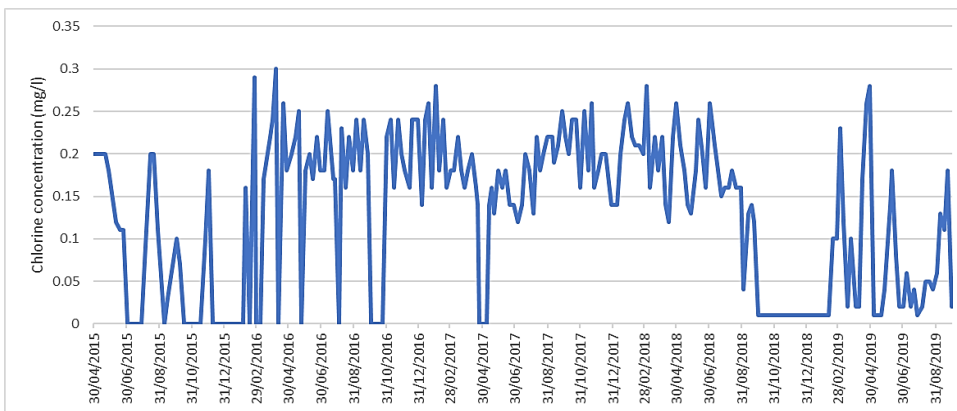
Source: SSE, 2020

Free chlorine measurements have been made at the outfall location by SSE over several years and continue to be made on a weekly basis. These data have provided information used to define the concentration of chlorine in the tracer used in the model. As with other parameters and assumptions applied in this modelling study, a conservative approach has been taken. Figure 5.2 shows the free chlorine concentration in the power station cooling water discharge for 50 months between 30 April 2015 to 31 August 2019. Typically, the average concentration is approximately 0.2mg/l with period when the concentrations are much lower. However, there are some period when concentrations reach 0.3mg/l and thus to be conservative a chlorine concentration of 0.3 mg/l has been used to define the outfall discharge properties in all model runs, which is the emission limit value under the current licence.

In the model the outfall flow rate is defined as 30,404 m<sup>3</sup>/hour (8.33m<sup>3</sup>/s, which corresponds to the working flow rate for the outfall as provided by the client. For continuity, this flow rate has also been applied to the cooling water intake as a negative flow rate. The chlorine concentration in the outfall is adjusted dynamically in the model to ensure the discharge concentration remains at 0.3mg/l above the concentration brought in through the cooling water system intake. This allows for the possibility of recirculation of the chlorine concentrations which could then increase above the 0.3mg/l added to the outfall discharge.

As part of the intake system, there is a fish pass which discharges abstracted water through the SW8 outfall on the southwest point on the power station where the estuary turns northward. . The outflow is a constant 20m<sup>3</sup>/hour, which equates to 0.006m<sup>3</sup>/s, approximately 0.07% of the main outfall flow rate. It is located over 400m to the west of the main outfall, the flow changes due to the outfall to the background flow conditions are negligible and therefore this SW8 outfall is not included in the simulations.

**Figure 5.2: Free Chlorine concentration in the outfall discharge (mg/l)**



Source: SSE, 2020

### 5.3 Sensitivity to chlorine decay

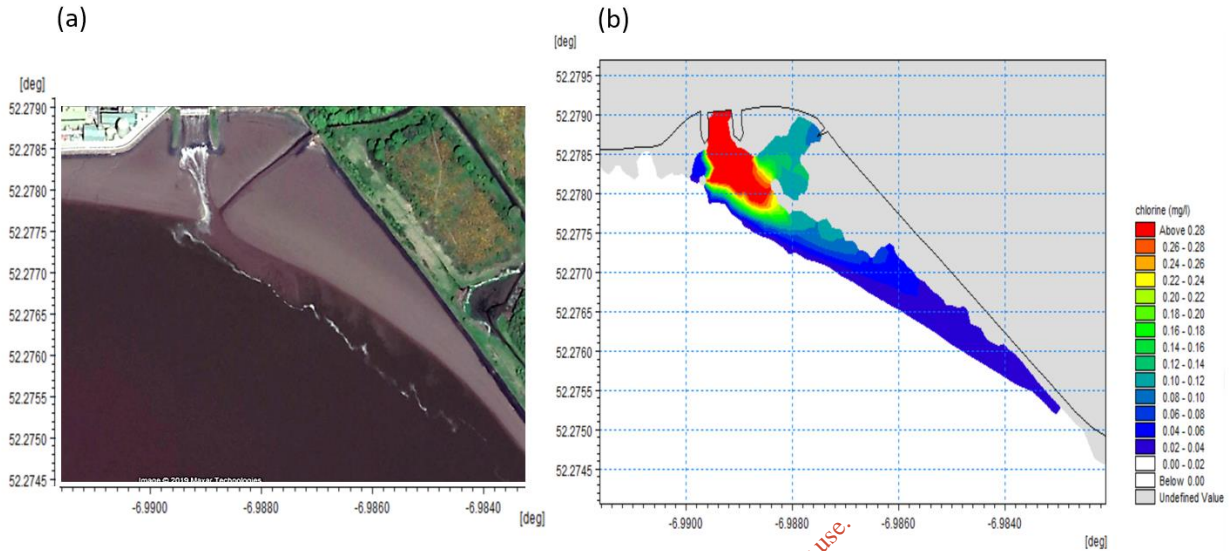
As the cooling water mixes and dilutes with the estuarine water, the concentration of chlorine declines with time. In addition, chlorine is affected by sunlight, and it reacts with sediments, other chemicals in the water and with biological processes in the aquatic environment. These processes result in additional chlorine loss over and above that attributed to dilution alone. As such, the decay of the chlorine compound in water is highly variable (e.g T90 can vary from a few hours to a couple of days) and is dependent upon a range of factors.

Model sensitivity tests were undertaken with varying degrees of decay rate applied to the chlorine released into the model. While the assumed decay did reduce the concentration of the chlorine, it appeared that in all areas except those relatively close to the outfall, the dispersion and associated dilution of chlorine in the plume, occurred faster than any imposed decay effects. For that reason, the model simulations reported here did not account for any decay in the chlorine released into the model. Were decay of chlorine to be incorporated into the model, the concentrations of chlorine would be lower. Thus, from the standpoint of chlorine dispersion simulation, the approach used is conservative.

### 5.4 Initial test of model performance

Results from initial model runs were compared visually with available aerial imagery of the cooling water plume. An example of an inter-comparison between aerial imagery and the model prediction of the cooling water outfall plume during the latter stages of the ebb tide is shown in Figure 5.3. The model is shown to reproduce well the spatial extent of the plume which in this case tends to cling to the eastern shore of the estuary to the south of the outfall. It shows also the rapid decrease in free chlorine concentration from around 0.3mg/l close to the out fall to values < 0.1mg/l at approximately 100m from the outfall.

**Figure 5.3: Visual comparison between aerial imagery and the model prediction of the cooling water outfall plume during the latter stages of the ebb tide**



Source: MML, 2020

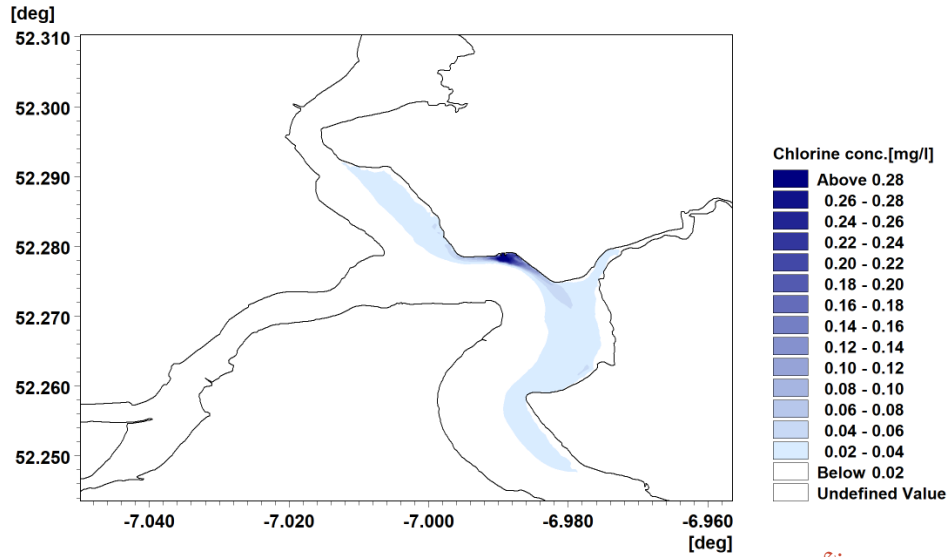
## 5.5 Neap tide simulation

The simulation of the chlorine dispersion from the outfall was undertaken during eight neap tides, the same period shown in Figure 4.6. The first model *warm-up* tide was discounted from the analysis, and the following seven tides have been considered in the subsequent analysis.

With the effect of the buoyancy of the warm cooling water discharge it was expected that the highest concentrations of the chlorine tracer would be experienced in the surface waters, and the lowest toward the seabed and thus the analysis of model output considers only the surface (layer 10) and bottom (layer 1) layers of the model. The analysis undertaken considered the maximum and mean chlorine concentrations, as well as the percentage of time during the simulation that three concentrations of chlorine defined as 0.05, 0.1 and 0.2 mg/l were exceeded.

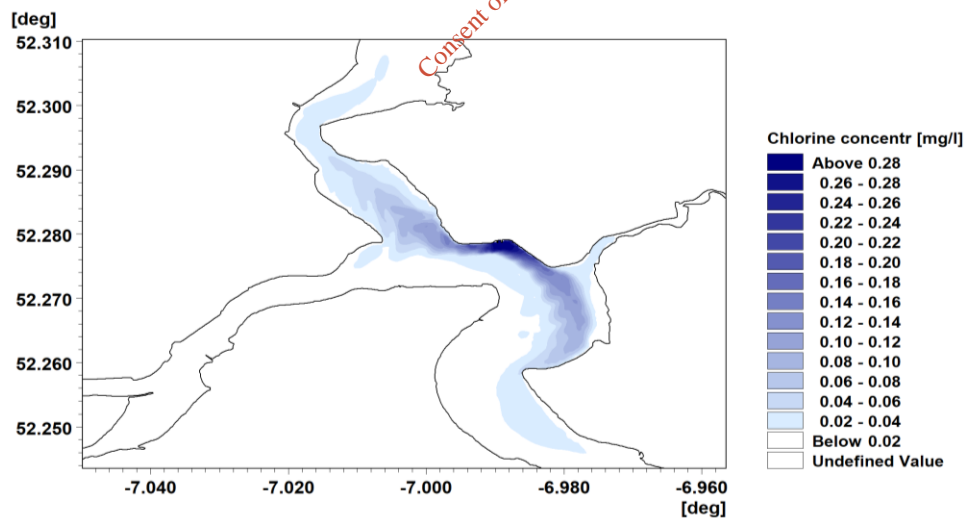
The maximum chlorine concentrations for the bottom and surface layers can be seen in Figure 5.4 and Figure 5.5, respectively. These figures show that over the seven simulated tides the mean concentration greater than 0.02mg/l is constrained within 650m of the outfall. For the maximum concentrations at the same 0.02mg/l threshold, the plume is constrained within 4.5km downstream of the outfall, and 4km upstream. Chlorine concentrations of 0.1mg/l do not extend beyond 2km downstream, and 800m upstream (surface layer).

**Figure 5.4: Bottom Layer: maximum chlorine concentrations (mg/l) throughout neap tides**



Source: MML, 2020

**Figure 5.5: Surface Layer: maximum chlorine concentrations (mg/l) throughout neap tides**



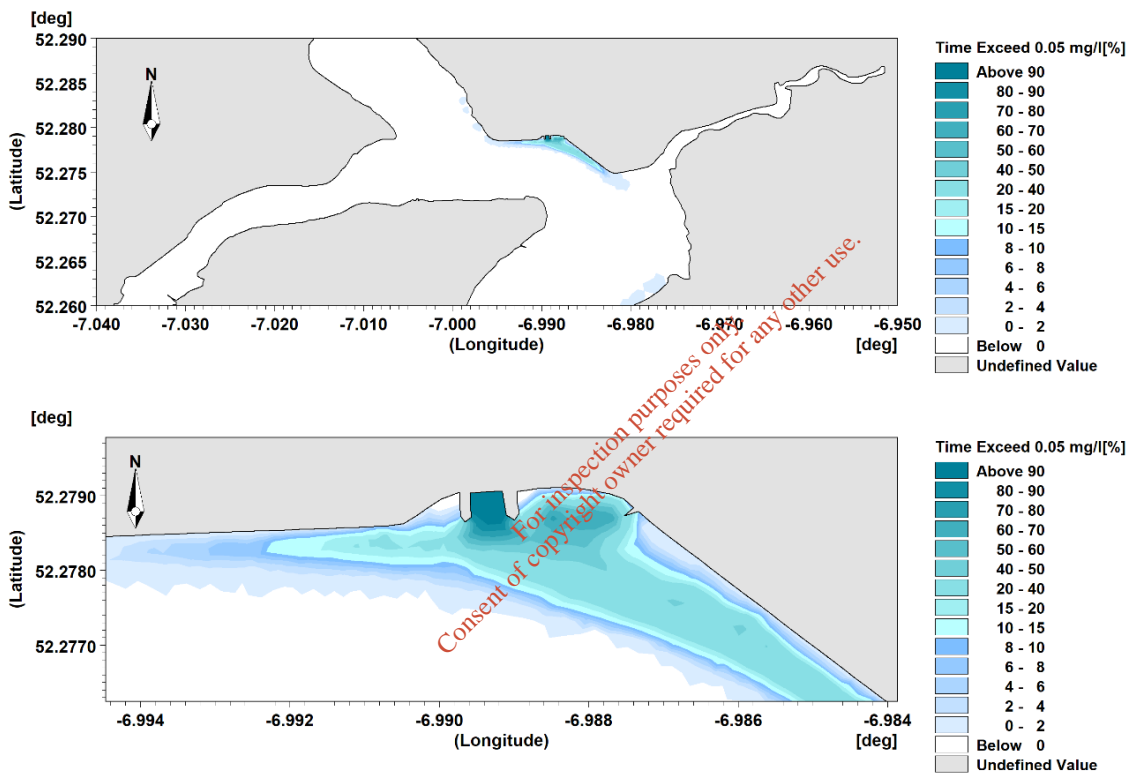
Source: MML, 2020



The results shown in Figure 5.4 and Figure 5.5 do not provide any indication of the time that the chlorine concentrations stay above a particular concentration level. To address this the model results were post-processed to calculate the percentage of time the chlorine exceeded 0.05, 0.1 and 0.2mg/l concentrations. It is noted that this was undertaken for the only the worst-case neap tides.

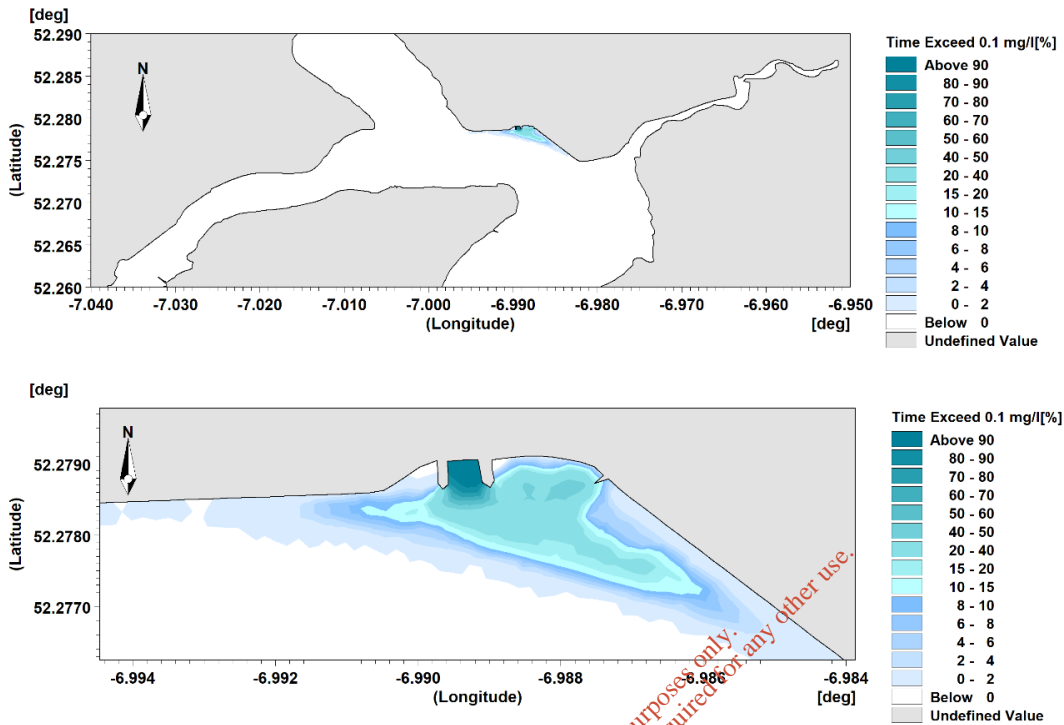
The percentage of time chlorine concentrations exceed 0.05, 0.1 and 0.2mg/l in the bottom layer of the model is shown Figure 5.6, Figure 5.7, and Figure 5.8 respectively. Figure 5.9, Figure 5.10: and Figure 5.11 show the same for the model surface layer.

**Figure 5.6: Bottom layer: percentage of time chlorine concentration exceeds 0.05mg/l**



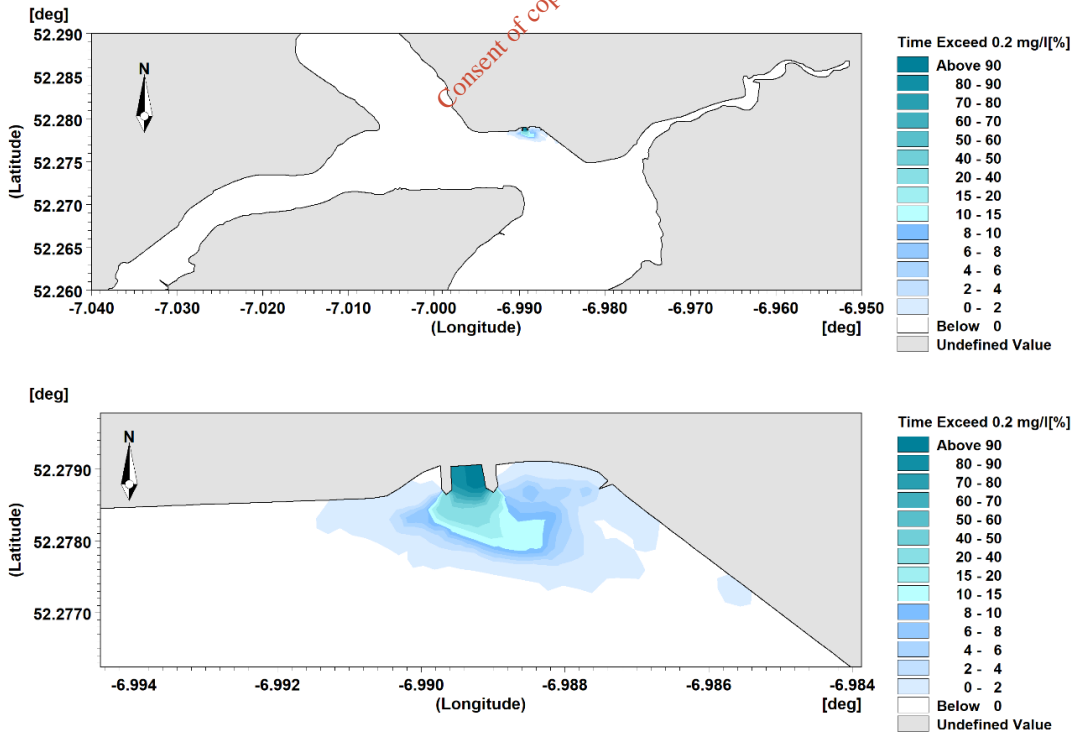
Source: MML, 2020

**Figure 5.7: Bottom layer: percentage of time chlorine concentration exceeds 0.1mg/l**



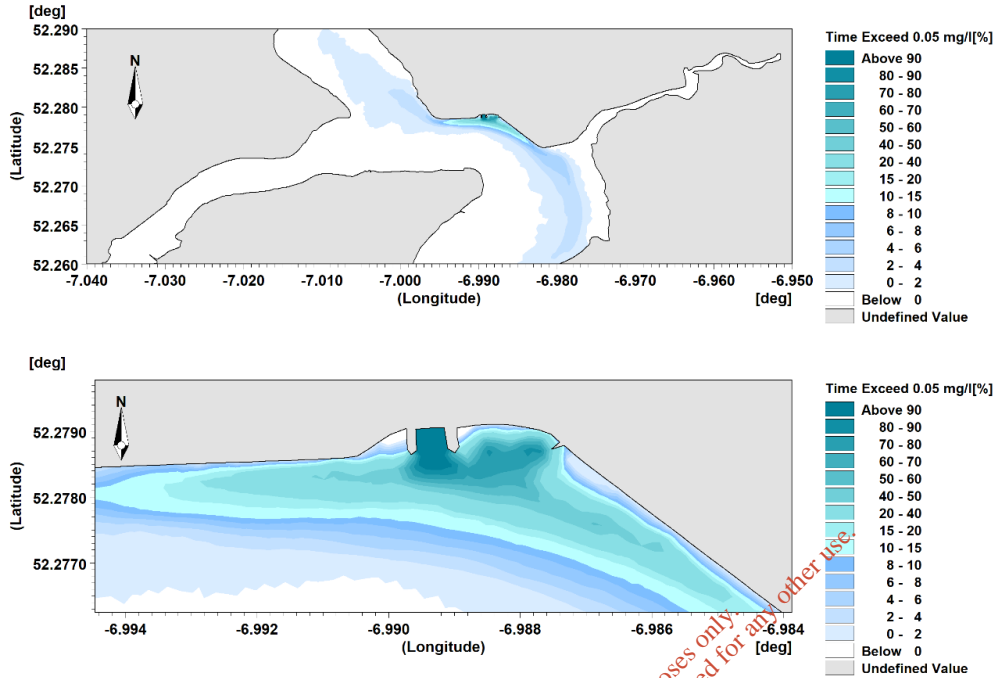
Source: MML, 2020

**Figure 5.8: Bottom layer: percentage of time chlorine concentration exceeds 0.2mg/l**



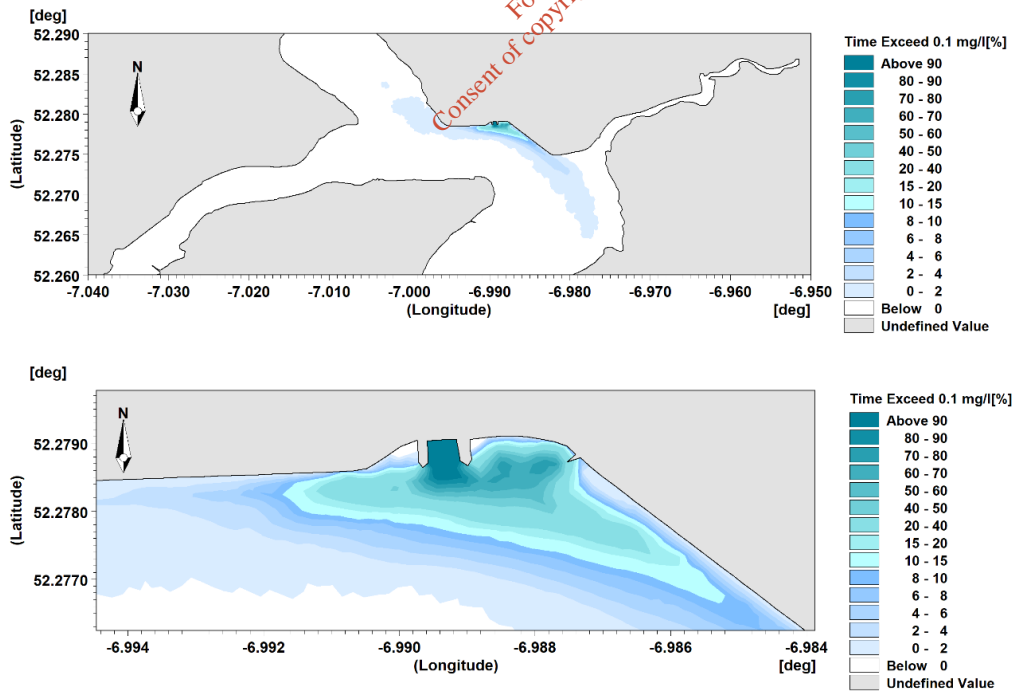
Source: MML, 2020

**Figure 5.9: Surface layer: percentage of time chlorine concentration exceeds 0.05mg/l**



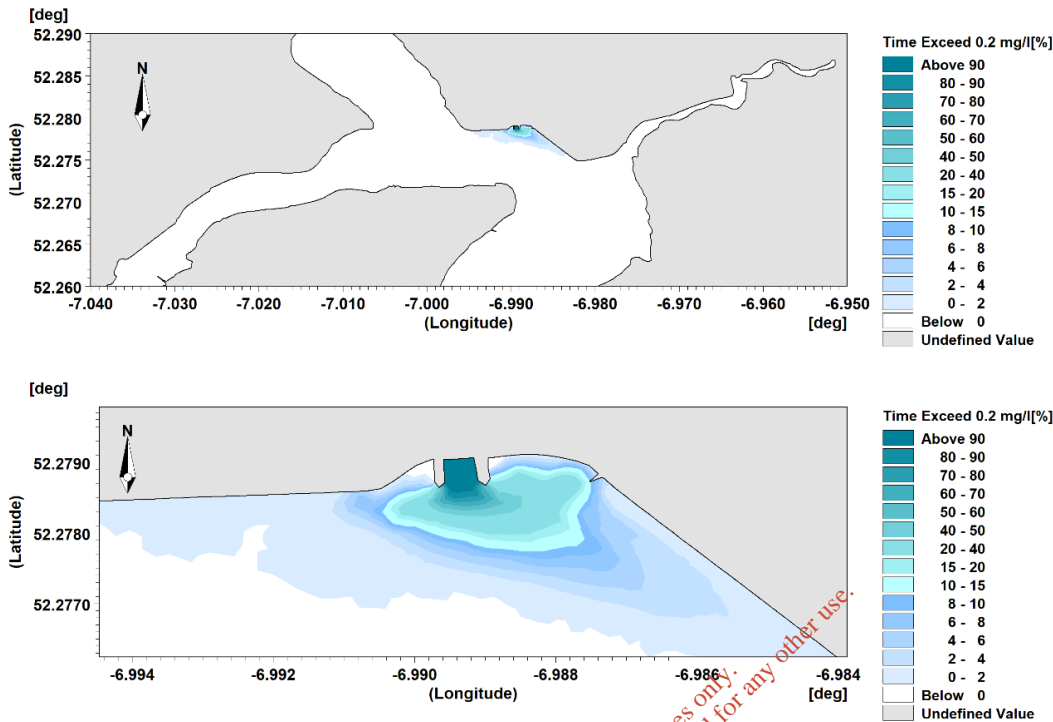
Source: MML, 2020

**Figure 5.10: Surface layer: percentage of time chlorine concentration exceeds 0.1mg/l**



Source: MML, 2020

**Figure 5.11: Surface layer: percentage of time chlorine concentration exceeds 0.2mg/l**



Source: MML, 2020

While Figure 5.5 shows that the model predicts maximum chlorine concentrations of 0.1mg/l extending 2km downstream from the outfall, Figure 5.11 demonstrates that this occurs for less than 2% of the time. The cooling water ponds at high water when current speeds are very low, it then moves downstream as a pool whilst mixing with the surrounding water. As the ebb tide reaches its peak the pond of water has dispersed and a plume with lower concentrations is formed, with the 0.1mg/l contour only reaching 300m downstream.

Together, the model results presented here show that the concentration of chlorine released from the cooling water outfall falls rapidly from the discharge location due to effective dispersion and dilution in the estuarine water. Natural decay of the chlorine, which was not included in the model, would reduce chlorine concentration and prevent any temporal increases in chlorine concentration associated with the continuous discharge of the cooling water and any cooling water recirculation effects.

## 5.6 Field data collection and analysis

Measurements of Chlorine concentrations and pH were obtained within the estuary at three locations on the morning of the 28<sup>th</sup> of January. This time and date were selected to capture conditions during the ebb phase of the tide when the plume from the power station extended the greatest distance to the south.

Table 5.1 shows the results from the measurements of chlorine concentration and pH. The pH across all three samples was recorded as 7.9. This indicates that there is no effect on pH as a result of the outflow. Chlorine concentrations at sample site A and B were both below the limit of detection for Chlorine. Sample point C had a slightly higher concentration at 0.09mg/l. Further information on this is provided in Appendix A..

**Table 5.1: Results from the measurements at sites A, B and C on 28<sup>th</sup> Jan 2020**

	Sample A	Sample B	Sample C
Time	10:18 UTM	10:46 UTM	10:05 UTM
Latitude	52° 16.410'N	52° 16.38'N	52° 12.28'N
Longitude	06° 59.200'W	06° 59.412'W	06° 57.608'W
Chlorine (Total, mg/l)	<0.05	<0.05	0.09
pH	7.9	7.9	7.9
Temperature (°C)	9	10	9

For inspection purposes only.  
Consent of copyright owner required for any other use.

## 6 Modelling pH

### 6.1 Introduction

The potential of Hydrogen (pH) expresses the concentration of hydrogen ions (H+) in a liquid in the form

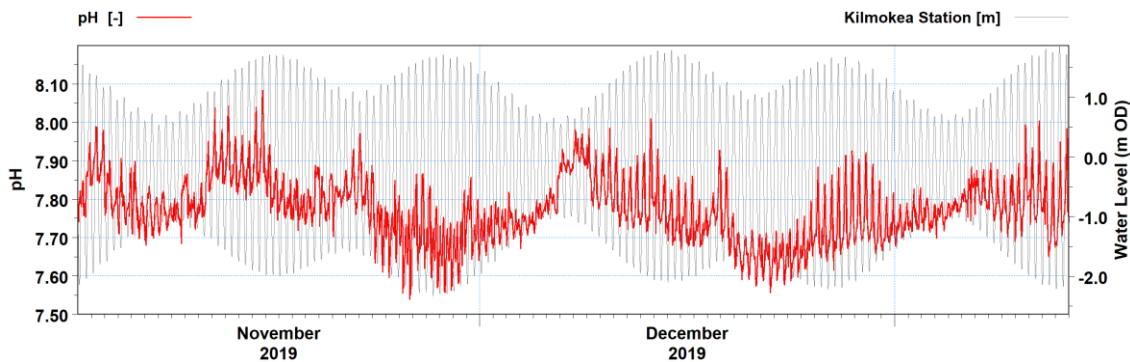
$$\text{pH} = -\log_{10}(c) \tag{1}$$

where c is hydrogen ion concentration in moles per litre. The minimum and maximum values on the pH scale are 0 and 14 with 0 defining the strongest acid and 14 defining the strongest alkaline. Pure water at room temperature (25°C) has a pH of 7.0 and is considered to be neutral.

Measured pH at the power station outfall, and water level at Kilmokea, is shown in Figure 6.1 for the period November to December 2019. It is noted that the measured pH indicates that the discharged cooling water is slightly alkaline and varies between 7.5 to 8.1 at the outfall. While there is a weak tidal modulation of the pH signal, there is no evidence of a correlation between pH values and the tidal spring-neap cycle. Figure 6.2 shows the same pH data from the power station outfall, with the addition of the EPA measurements of pH and the river flow. It can be seen that the EPA measurements at a location adjacent to the power station (EPA site SR510), pH values between about 7.9 and 8.1 have been measured. What is evident is that the EPA measurements were made during periods of low river flow. It can be seen in the power station pH measurements that there is a reduction in pH during and immediately after higher river flows, with values dropping to a pH value of 7.6. However, it can also be seen that during periods of low river flow, the measurements in the outfall water are of a similar magnitude to that of the EPA measurements during similar low river flow.

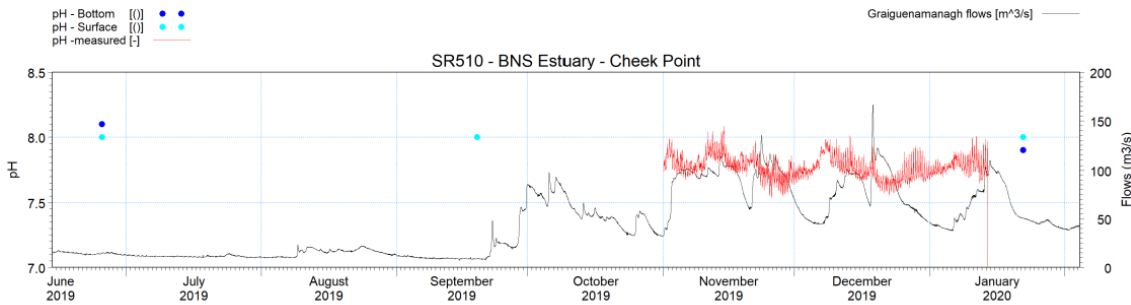
Figure 6.3 shows the pH measurements upstream of New Ross in the upper reaches of the estuary. It can be seen that during periods of high river flow, pH measurements drop down to about 7.2 in 2018/2019. This suggests that the river water has a lower pH than the estuary water. The model has assumed that the river water has a neutral pH of 7.0 and is thus both conservative and consistent with the available data.

**Figure 6.1: Measured pH at the power station outfall, and water level at Kilmokea for the period November to December 2019**



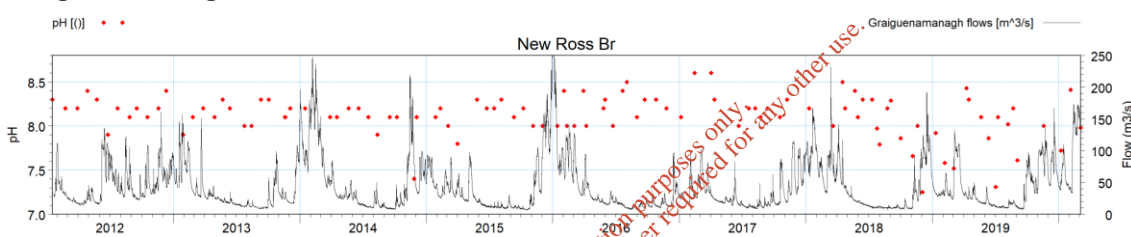
Source: SSE & MML, 2020

**Figure 6.2: Measured pH at the power station outfall, EPA measurements of pH and river flows at Graiguenamanagh**



Source: SSE & MML, 2020

**Figure 6.3: EPA measured pH values upstream of New Ross and river flows at Graiguenamanagh**



In the pH dispersion modelling to access pH conditions at the site, pH was modelled as a concentration (c) using Equation 2 and the model results were converted back to pH using Equation 1 in the form

$$c = 10^{-\text{pH}} \quad (2)$$

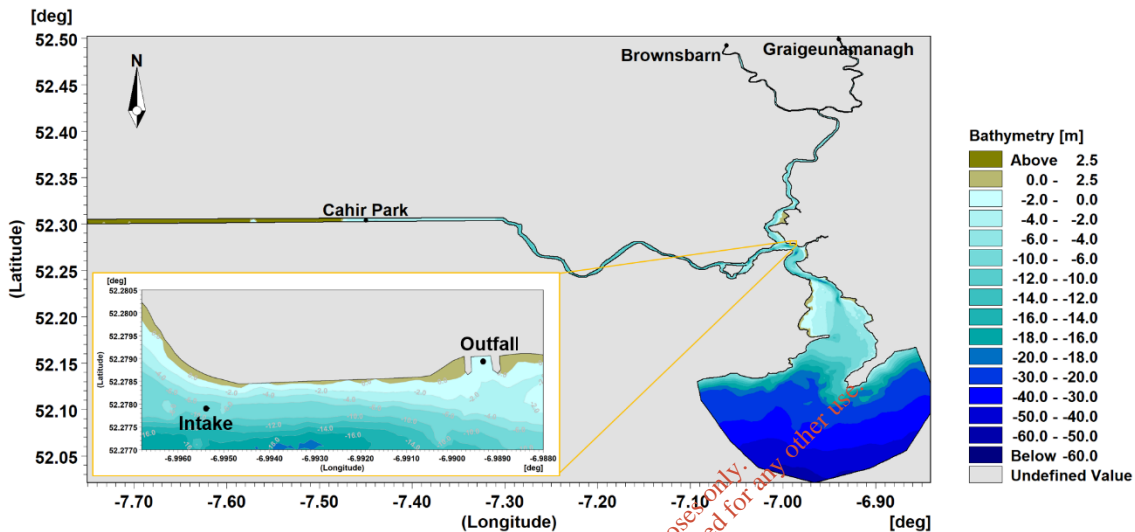
## 6.2 Model setup

The MIKE3 FM HD model provided the tidal variations in water levels and currents throughout the estuary utilised in the pH dispersion model. The pH at five locations were defined using H<sup>+</sup> concentration values in the pH dispersion model. As measured pH was only available at the outfall (Figure 6.1), this information was used to supply pH as a source in the model. The H<sup>+</sup> concentration values used at the stated locations in the model are summarised in Table 6.1. Table 6.1: shows that the pH at the outfall and intake was set as 8 while pH of 8.1 was supplied at the open boundary and initial condition. These are conservative assumptions and are considered to be representative of the worst-case scenario.

It should be noted that whilst there are measurements of pH values throughout the estuary obtained by the EPA, the majority of these measurements occur outside periods of high freshwater flow and there are no measurements of pH throughout a tidal cycle available to calibrate the model. Model results presented here therefore tend to show lower pH values (due to the higher freshwater flow), especially at or close to low water, than those measured by the EPA. While, the pH time-series data from the power station outfall shows a greater variation in

pH, the cooling water is abstracted from the intake in deeper water. It is considered that these measurements may not always account for the lower pH values that might be expected in the fresher, lower pH water, ebbing out of the estuary after high water. This does not negate the pH modelling since it has been demonstrated that the pH of the outfall discharge into the receiving waters is correctly simulated as it is using the same dispersion parameters as for the chlorine simulation.

**Figure 6.4: Source locations in the pH modelling study**



Source: MML, 2020

**Table 6.1: pH model inputs**

Location	pH	Concentration H <sup>+</sup>
Outfall	8.0	$1.00 \times 10^{-8}$
Intake	8.0	$1.00 \times 10^{-8}$
Graigeunamanagh	7.0	$1.00 \times 10^{-7}$
Brownsbarn	7.0	$1.00 \times 10^{-7}$
Cahir Park	7.0	$1.00 \times 10^{-7}$
Initial Condition	8.1	$7.94 \times 10^{-9}$
Offshore Boundary	8.1	$7.94 \times 10^{-9}$

## 6.3 pH results

### 6.3.1 Spatial distribution

The pH model results were analysed to provide spatial and temporal quantification of water pH in the Barrow estuary in the surface and bottom layers. The spatial distribution of pH values for the high and low water in the surface water layer in the vicinity of the power station outfall is shown in Figure 6.5 and Figure 6.6, respectively. These figures show that water with a pH around 8.0 is confined to a relatively small area around the outfall.

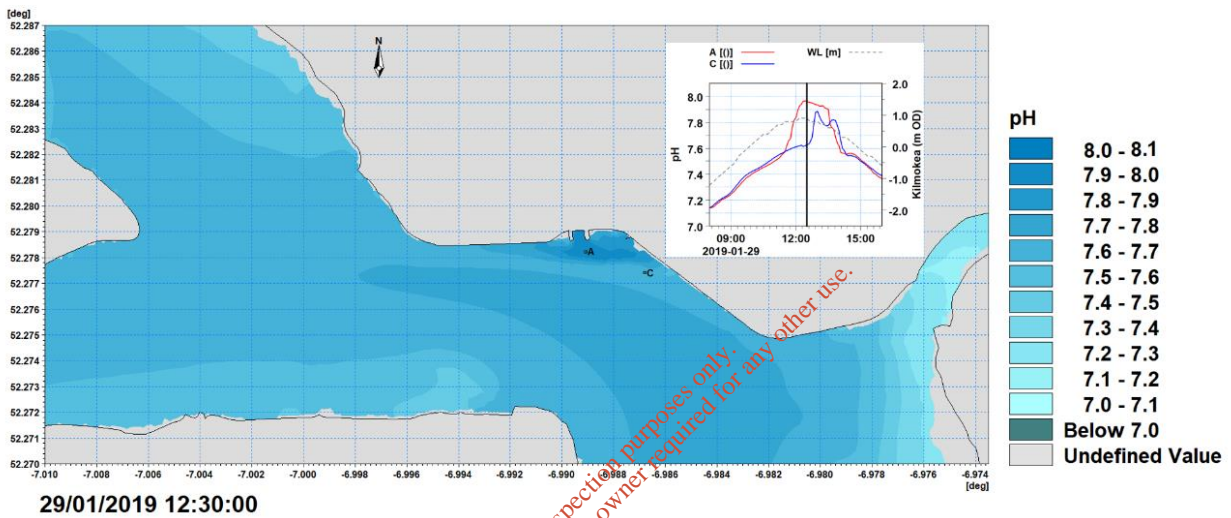


### 6.3.2 Temporal distribution

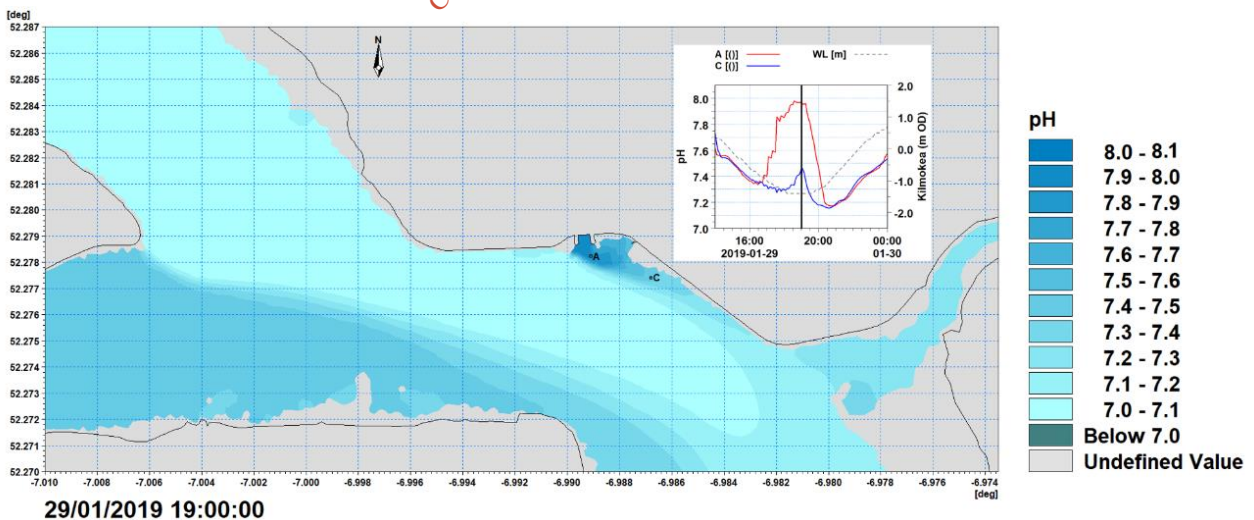
#### Surface layer

The temporal variation of water pH was also examined at two locations; A (close to the outfall) and; C, approximately 300m to the south east of the outfall (Figure 6.5). During high water Figure 6.5: shows that pH at surface layer was 7.9 and 7.6 at A and C, respectively. In contrast, in Figure 6.6 it shows pH at C during low water was lower (7.45) whereas pH at A was similar to pH during high water.

**Figure 6.5: Spatial pH variation in the surface layer during high water level near the power station outfall.**



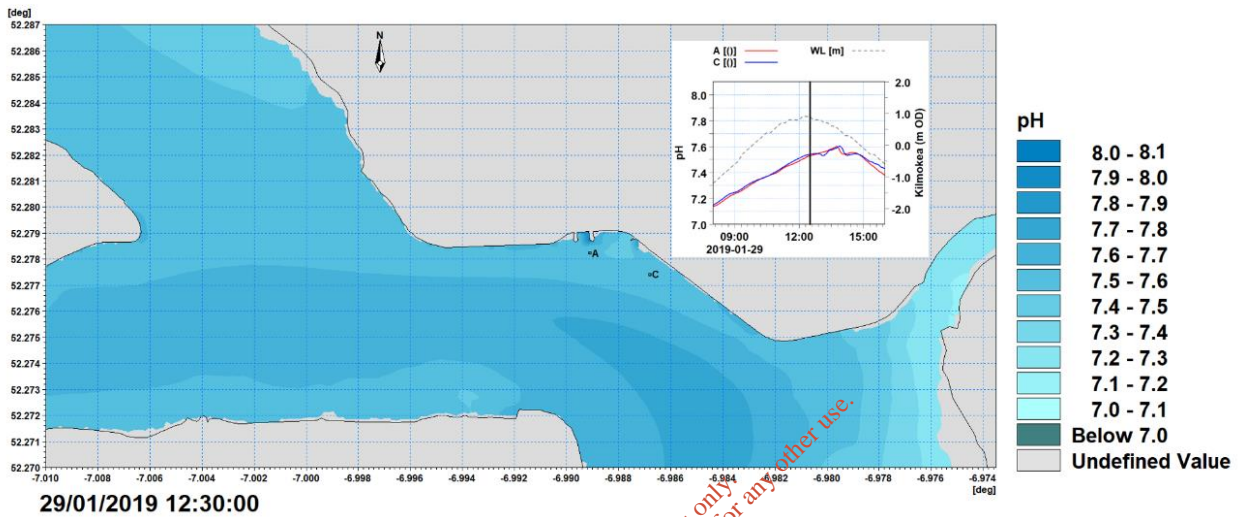
**Figure 6.6: Spatial pH variation in the surface layer during low water level near the power station outfall.**



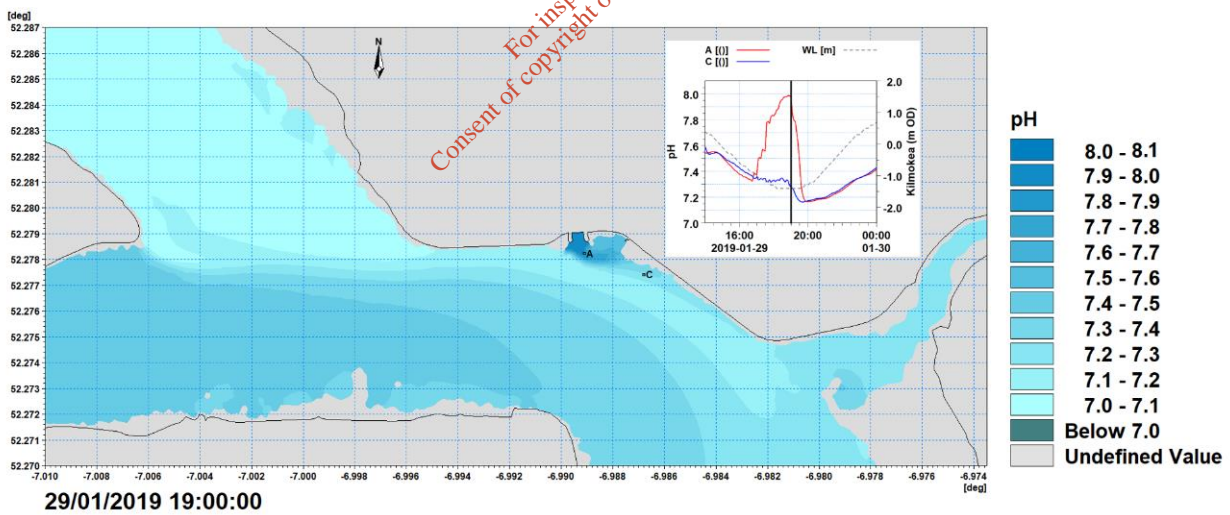
### Bottom layer

Figure 6.7 and Figure 6.8 shows water pH at the bottom layer with temporal pH values at A and C during high and low water, respectively. It is observed that pH was 7.5 at A and C location during high water at the bottom layer (Figure 6.7) while during low water, pH was 7.9 and 7.3 at A and B, respectively (Figure 6.8).

**Figure 6.7:: Overview of pH variation at bottom layer during high water level.**



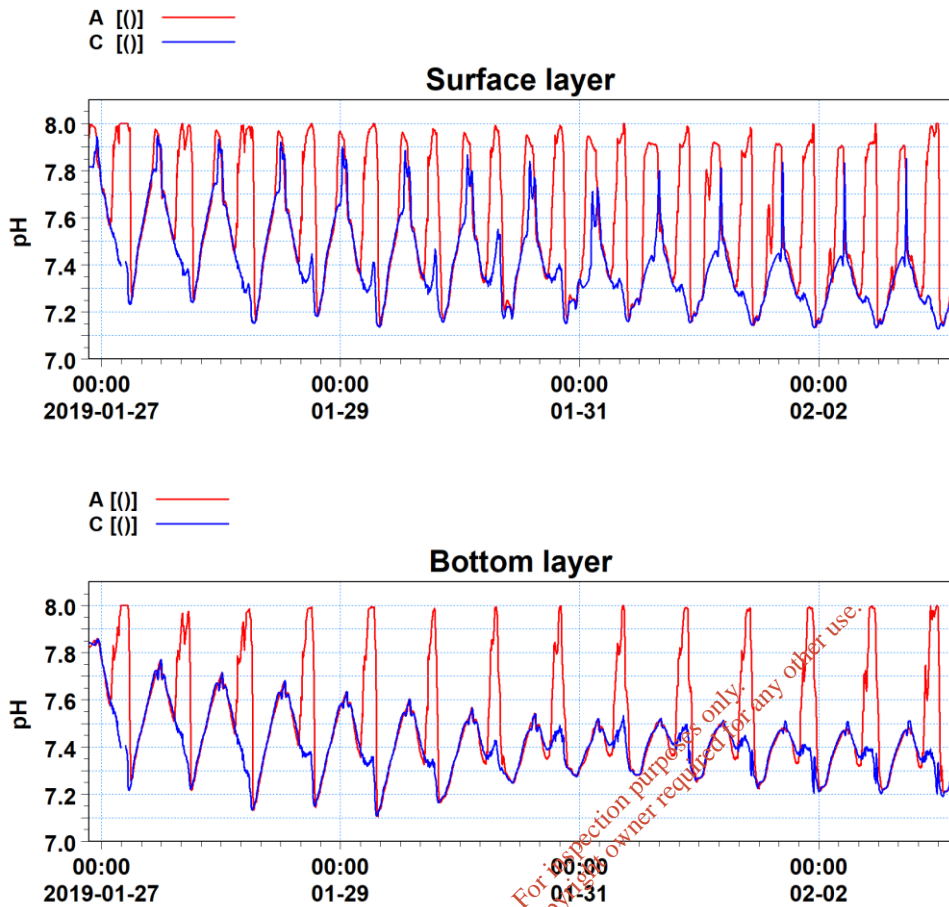
**Figure 6.8: Overview of pH values at bottom layer during low water level.**



Source: MML, 2020

To examine in more detail the temporal variation in pH predicted by the model, a time-series of pH at A and C is shown in Figure 6.9 for the surface and bottom layers. It is observed that pH at A and C was higher during flood and ebb tide at the bottom and surface layer due to the influence of flow discharge at the outfall. However, the results show that these values are within the range of the measured pH at the outfall (i.e. 7.5 to 8.1). Figure 6.9 also demonstrates that the model simulated the worst-case scenario and thus provide conservative results.

**Figure 6.9: pH values at A and C at the surface and bottom layer.**

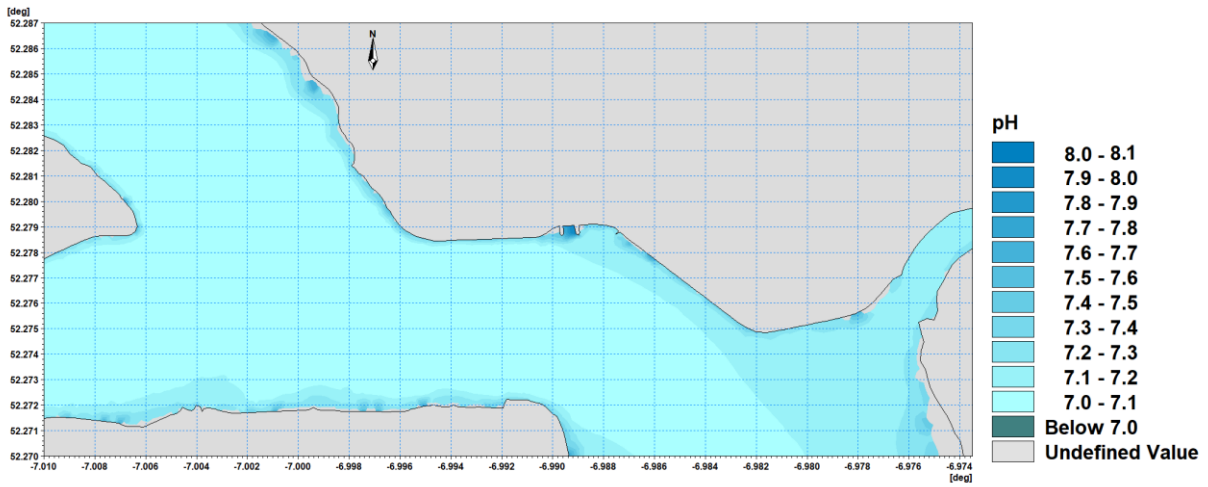


Source: MML, 2020

Data describing the spatial distribution of the short-term maximum pH at the surface and bottom layers were also extracted from the model and are shown in Figure 6.10 and Figure 6.11, respectively. These maximum pH values of 8 occur temporarily during periods of slack water during the tidal cycle. The spatial extent of water with a pH of 8 is confined to less than 100m from the outfall location and persists for only a short time during slack water. Subsequent ebb or flood tidal flows rapidly disperse the plume and reduce the pH to values close to the ambient estuarine water values. Based on pH modelling results, it is demonstrated that the pH values at the site are not varying much and this indicates that pH is essentially unaffected by chlorine dosing.

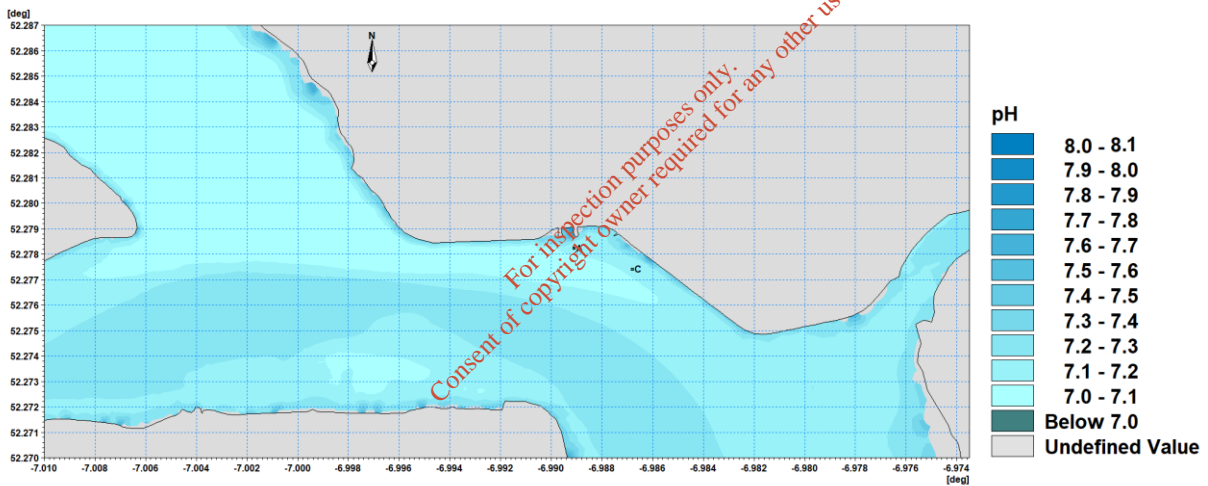
The natural variability of pH captured in the EPA data varies between approximately 7.9 and 8.2 according to the measurements at EPA location SR510 (Cheekpoint) and SR520 (Buttermilk Point). At the Campile location (D0409- SW1-DS) the pH varies between 7.2 to 8.6. The results from the pH modelling show that the pH values from the outfall plume fall within the natural variation of pH shown in the EPA measurements, and therefore any organisms living in the vicinity of the Great Island power station will already be adapted to changes of pH between 7.9 to 8.2, as well as lower pH values arising during periods of heavy rainfall and subsequent high river flows.

Figure 6.10: Maximum short-term pH values at surface layer.



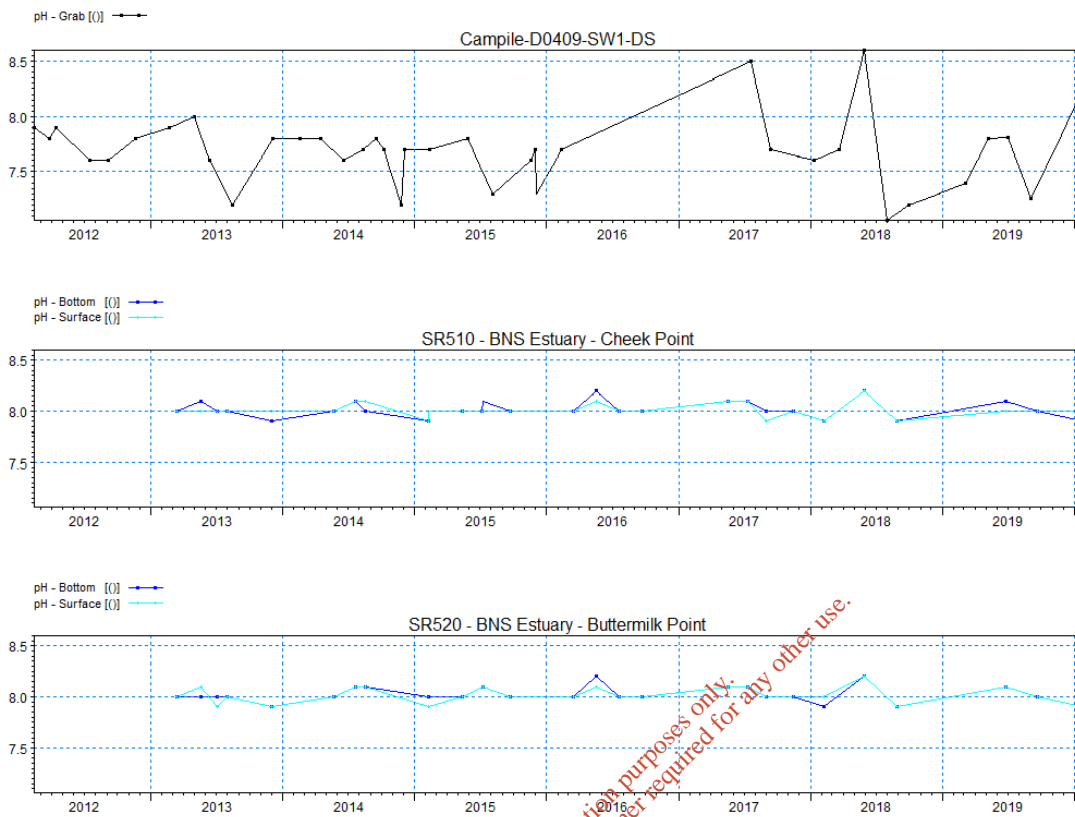
Source: MML, 2020

Figure 6.11: Maximum short-term pH values at bottom layer.



Source: MML, 2020

**Figure 6.12: EPA pH measurements at three locations close to the Great Island Power Station**



For inspection purposes only.  
Consent of copyright owner required for any other use.

## 7 Biological Effects

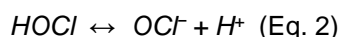
### 7.1 Characteristics of NaOCl in the marine environment

The use of seawater as a coolant in power stations introduces the risk of biofouling as organisms such as barnacles, oysters, bryozoans, algae and bacteria can colonise surfaces within the system. If left to grow unhindered these organisms can compromise plant efficiency, reliability and safety. Sodium hypochlorite (NaOCl) is widely used to disinfect seawater in power plant cooling systems and prevent or reduce biofouling (Saleem et al., 2012).

When NaOCl is added to water it dissociates rapidly into sodium hydroxide (NaOH) and free chlorine in the form of hypochlorous acid (HOCl), as shown in Eq. 1.



Hypochlorous acid further dissociates into hydrogen ions (H<sup>+</sup>) and hypochlorite ions (OCl<sup>-</sup>), as shown in Eq. 2.



The dissociation of HOCl is reversible and strongly dependent on pH (Sarbatly and Krishnaiah, 2007). Generally, the proportion of HOCl increases as pH decreases (Sugam and Helz, 1976). For example, in seawater at 20°C and 30 PSU, HOCl will account for 99 % of free chlorine at pH 5.2, and OCl<sup>-</sup> will account for approximately 99 % of free chlorine at pH 9.3. At pH 7.5 half of the free chlorine is active as HOCl and half is available as OCl<sup>-</sup>. HOCl is 80 to 200 times stronger than OCl<sup>-</sup> in terms of pathogen disinfection, which likely also means that it has a stronger biocidal effect on target organisms in power station cooling systems and on non-target organisms in the receiving aquatic environment.

Hypochlorite will not reach the aquatic environment via power station cooling water discharge due to the high reactivity and rapid dissociation of NaOCl when added to seawater in cooling systems (Binetti and Attias, 2009). Free chlorine compounds, HOCl and OCl<sup>-</sup>, are also often short-lived and subsequent reactions are typically bromine based given the abundance of bromide in seawater. Free chlorine compounds react with bromide ions (Br<sup>-</sup>) in seawater to form hypobromous acid (HOBr) and hypobromite ions (OBr<sup>-</sup>), as shown in Eq. 3.



In turn, free bromine and chlorine compounds react with organic and mineral constituents of seawater to produce a complex mixture of halogenated compounds, including trihalomethanes (e.g. chloroform and bromoform), haloacetonitriles, haloacetic acids and halophenols (Jenner et al., 1997; Khalanski, 2002). These chlorination by-products (CBPs) are less effective than free chlorines as a disinfectant, but their action continues for a longer time. Many CBPs are persistent in natural aquatic environments and have been proven to be, or are suspected of being, toxic to humans and animals when subject to long-term exposure (BEEMS Expert Panel, 2010). Free chlorines and CBPs are collectively known as residual chlorine or residual oxidant.

NaOCl dissipates rapidly on contact with soil and sediments (DT50 < 1 minute) and does not have a high potential to adsorb to sediments (European Chemicals Agency, 2019). Studies concerning the contamination of estuarine sediments with CBPs are scarce. A recent study investigated the occurrence and distribution of CBPs in sediments in the Gulf of Fos (Marseille, France), a semi-enclosed bay to which chlorinated effluents from multiple industrial plants are

discharged (Manasfi et al., 2018). Bromine-containing halophenols were detected in sediment samples, which was consistent with the speciation of CBPs in seawater samples from the bay and therefore suggestive of adsorption of CBPs into marine sediments or contamination via the sedimentation of CBPs accumulated in organic matter.

## 7.2 Ecology of Barrow Estuary

### 7.2.1 Site designations and features of conservation importance

The Great Island CCGT Power Station discharges cooling water into the River Barrow and River Nore Special Area of Conservation (SAC; site code: 2162). The area is also proposed as a Natural Heritage Area (NHA). The SAC consists of the freshwater stretches of the Barrow and Nore River catchments as far upstream as the Slieve Bloom Mountains, and it also includes the tidal elements and estuary as far downstream as Creadun Head in Waterford. The site is designated as a SAC for the following habitats and species listed under Annex I/II of the EU Habitats Directive (Council Directive 92/43/EEC on the Conservation of natural habitats and of wild fauna and flora) and for birds listed under Article 4 of the EU Birds Directive (Council Directive 2009/147/EC on the conservation of wild birds).

**Table 7.1:: River Barrow and River Nore SAC habitats listed under Annex I of the EU Habitats Directive (\* = priority)**

Habitat type	Natura 2000 Code	Cover (ha)
Estuaries	1130	3856.36
Tidal mudflats and sandflats	1140	925.69
Reefs	1170	123.73
<i>Salicornia</i> mud	1310	0.03
Atlantic salt meadows	1330	34.75
Mediterranean salt meadows	1410	0.12
Floating river vegetation	3260	123.73
Dry heath	4030	123.73
Hydrophilous tall herb communities	6430	123.73
Petrifying spring *	7220	123.73
Old oak woodlands	91A0	75.08
Alluvial forests*	91E0	110.07

Source: Adapted from the Natura 2000 Standard Data Form, 2017.

**Table 7.2: River Barrow and River Nore SAC species listed under Annex II of the EU Habitats Directive**

Common name	Scientific name	Natura 2000 code	Group	Type	Abundance category
Desmoulin's whorl snail	<i>Vertigo moulinsiana</i>	1016	Invertebrates	Permanent	Present
Freshwater pearl mussel	<i>Margaritifera margaritifera</i>	1029	Invertebrates	Permanent	Present
Nore freshwater pearl mussel	<i>Margaritifera durrovensis</i>	1990	Invertebrates	Permanent	Very rare
White-clawed crayfish	<i>Austropotamobius pallipes</i>	1092	Invertebrates	Permanent	Present
Sea lamprey	<i>Petromyzon marinus</i>	1095	Fish	Reproducing	Present

Common name	Scientific name	Natura 2000 code	Group	Type	Abundance category
Brook lamprey	<i>Lampetra planeri</i>	1096	Fish	Permanent	Present
River lamprey	<i>Lampetra fluviatilis</i>	1099	Fish	Reproducing	Present
Twaite shad	<i>Alosa fallax</i>	1103	Fish	Reproducing	Present
Atlantic salmon	<i>Salmo salar</i>	1106	Fish	Reproducing	Concentration
Otter	<i>Lutra lutra</i>	1355	Mammals	Permanent	Present
Killarney Fern	<i>Trichomanes speciosum</i>	1421	Plants	Permanent	Present

Source: Adapted from the Natura 2000 Standard Data Form, 2017.

**Table 7.3: River Barrow and River Nore SAC birds listed under Article 4 of the EU Birds Directive**

Common name	Latin name	Population type	Population minimum	Population maximum	Units
Kingfisher	<i>Alcedo atthis</i>	Reproducing	10	10	Pairs
Teal	<i>Anas crecca</i>	Wintering	1	471	Individuals
Widgeon	<i>Anas penelope</i>	Wintering	1000	1000	Individuals
Mallard	<i>Anas platyrhynchos</i>	Wintering	1	528	Individuals
Greenland white-fronted goose	<i>Anser albifrons ssp. Flavirostris</i>	Wintering	52	52	Individuals
Pochard	<i>Aythya ferina</i>	Wintering	1	83	Individuals
Goldeneye	<i>Bucephala clangula</i>	Wintering	1	10	Individuals
Sanderling	<i>Calidris alba</i>	Wintering	20	20	Individuals
Dunlin	<i>Calidris alpina</i>	Wintering	2212	2212	Individuals
Bewick's swan	<i>Cygnus columbianus ssp. Bewickii</i>	Wintering	31	31	Individuals
Mute swan	<i>Cygnus cygnus</i>	Wintering	76	76	Individuals
Peregrine	<i>Falco peregrinus</i>	Reproducing	1	1	Pairs
Oystercatcher	<i>Haematopus ostralegus</i>	Wintering	939	939	Individuals
Swallow	<i>Hirundo rustica</i>	Concentration	10000	10000	Individuals
Bar-tailed godwit	<i>Limosa lapponica</i>	Wintering	196	196	Individuals
Black-tailed godwit	<i>Limosa limosa</i>	Wintering	62	62	Individuals
Curlew	<i>Numenius arquata</i>	Wintering	1	826	Individuals
Golden plover	<i>Pluvialis apricaria</i>	Wintering	3500	3500	Individuals
Shelduck	<i>Tadorna tadorna</i>	Wintering	1	122	Individuals
Greenshank	<i>Tringa nebularia</i>	Wintering	3	8	Individuals
Redshank	<i>Tringa totanus</i>	Wintering	1	560	Individuals
Lapwing	<i>Vanellus vanellus</i>	Wintering	2141	2141	Individuals

Source: Adapted from the Natura 2000 Standard Data Form, 2017.

## 7.2.2 Estuarine benthic ecology

Barrow Estuary features extensive areas of good quality intertidal and subtidal flats, comprised of substrates ranging from fine, silty mud to coarse sand and pebbles. Benthic surveys were



undertaken in 2008 to determine macrofaunal and sediment distribution patterns in the River Nore and River Barrow Special Area of Conservation (Kennedy, 2008). The survey data were used to identify the following broad habitat and benthic community types downstream of the Great Island CCGT Power Station cooling water discharge point (National Parks and Wildlife Service, 2011):

- **Fine sand with *Fabulina fabula* community:** This subtidal community is confined to the southern margin of the SAC at the mouth of Waterford Harbour. Sediment ranges from very fine to fine, and the biological community is distinguished by moderately high abundances of both the bivalve *Fabulina fabula* and the polychaete worm *Nephtys hombergii*.
- **Muddy estuarine community complex:** This community complex is present in both the intertidal and subtidal zones. Substrate is predominantly of fine material and distinguishing species are the bivalves *Scrobicularia plana* and *Macoma balthica*, the amphipod *Corophium volutator*, the polychaete *Streblospio shrubsolii* and the oligochaetes *Tubificoides pseudogaster* and *Tubificoides benedii*. These species are indicative of a variable salinity community.
- **Sand to muddy fine sand community complex:** This community complex covers much of the estuary area downstream from the cooling water discharge point and occurs from the upper intertidal to the subtidal zone. Substrate represents a gradient from medium sand to silt-clay. The bivalve *Cerastoderma edule* and the polychaete *Scolelepis squamata* are common in courser sediments, and the bivalve *Macoma balthica* and the polychaete *Pygospio elegans* are more commonly present in areas of finer grained sediment.
- **Sabellaria alveolate reef:** This habitat type occurs intertidally in Duncannon Bay, on the eastern side of the estuary near the southern margin of the SAC. This biogenic reef forms draping structures over exposed bedrock and, where suitable substrate is available, forms upstanding features with a prominent three-dimensional aspect. A range of species inhabit these reefs, including: *Enteromorpha* sp., *Ulva* sp., *Fucus vesiculosus*, *Fucus serratus*, *Polysiphonia* sp., *Chondrus crispus*, *Palmaria palmate*, *Coralinus officinalis*, *Nemertea* sp., *Actinia equine*, *Patella vulgate*, *Littorina littorea*, *Littorina obtusata* and *Mytilus edulis*.

### 7.3 Literature review of chlorinated effluent impacts on ecological receptors

A search was conducted for peer-reviewed literature and reports relating to the impacts of chlorinated effluent on non-target organisms of receiving estuarine ecosystems. Key findings of the literature search are summarised in the following sub-sections. The implications of these data in relation to the outflow and the aquatic environment in the Barrow Estuary is then examined further in section 7.4.

#### 7.3.1 Plankton

Field and laboratory investigations have generally shown negative impacts of chlorination on phytoplankton. Ma et al. (2011) determined that growth of the marine diatom *Phaeodactylum tricorutum* was completely inhibited when exposed to free chlorine (i.e. HOCl and OCl<sup>-</sup>) concentrations of 0.20 mg/l for 24 hours; chlorophyll *a* and carotenoids contents of cells decreased 63 % and 61 %, respectively, over the treatment period. Zargar and Ghosh (2007) also reported that phytoplankton growth was inhibited when exposed to NaOCl solution. Growth of the green algae *Chlorella vulgaris* was adversely affected at chlorine concentrations ≥ 0.25 mg/l, when tested experimentally at temperatures ≥ 26°C. Lethal concentrations of free chlorine and CBPs to phytoplankton vary interspecifically. For example, the diatom *Skeletonema costatum* was killed when exposed to a chlorine concentration of 1.5 to 2.3 ppm for 5 to 10 minutes, whereas the green algae *Chlamydomonas* sp. was not irreversibly damaged when

exposed to chlorine concentrations of 20 ppm over the same time period (Hirayama and Hirano, 1970).

The impacts of chlorination on zooplankton appear to have largely been tested on freshwater species, rather than marine zooplankton species. Zargar and Ghosh (2007) investigated the impacts of chlorination on two freshwater zooplankton: Cladocera *Ceriodaphnia reticulata* and copepod *Cyclops viridis*. Chlorine levels of 0.25 and 0.5 mg/l were lethal to the zooplankton within 2 hours of exposure (at temperatures  $\geq 26$  °C). Similar results were found by Husnah and Lin (2002) for rotifers *Hexarthra* sp. and *Brachionus* sp. when the species were exposed to a chlorine concentration of 0.25 mg/l. Latimer et al. (1975) tested the toxicity of power station CBPs on copepods *Limnocalanus macrurus* and *Cyclops bicuspidatus thomasi*. The "safe" level of exposure was defined as the concentration at which mortality was  $\leq 5$  % of the test individuals over an exposure period of 30 minutes. Based on the results of bioassay experiments, the predicted "safe" CBP concentrations were 0.9 mg/l for *Limnocalanus macrurus* and 0.5 mg/l for *Cyclops bicuspidatus thomasi*. Benthic Ecology

### Macroalgae

Macroalgae do not possess a protective cuticle and are therefore highly susceptible to chemical damage. Kerrison et al. (2016) investigated the effect of a range of chemical disinfectants, including NaOCl, at different concentrations and exposure times on five species of macroalgae: *Palmria palmata*, *Osmundea pinnatifida*, *Ulva lactuca*, *Ectocarpus siliculosus* and *Ulva intestinalis*. The response to NaOCl exposure varied between species. *Ulva intestinalis* was the most sensitive species, exposure to a solution of 0.1 % NaOCl for 1 minute had a severe physiological effect and exposure for 1 minute to a 1 % solution of NaOCl had a lethal effect. Exposure to a 5 % NaOCl solution for one-minute had a lethal effect on all five macroalgae species. It should be noted that the range of NaOCl concentrations used in this experiment exceed environmentally relevant concentrations, including typical concentrations of NaOCl in power station cooling water. In addition, hypochlorite will not reach the aquatic environment via power station cooling water discharge due to the high reactivity and rapid dissociation of NaOCl when added to seawater in cooling systems (Binetti and Attias, 2009). However, the literature search did not return any studies specifically concerning the effects of chlorinated power station effluent on estuarine macroalgae.

### Macroinvertebrates

Bivalve molluscs are typically the dominant fouling organisms in coastal power station cooling water systems and are often the intended target of NaOCl dosing of cooling waters. Consequently, the impacts of seawater chlorination on bivalves have been relatively well studied compared to the impacts on other estuarine organisms.

Bivalve molluscs feed primarily by filter feeding and/or surface deposit feeding. These feeding processes mean that any contaminants within the water column or sediment have the potential to accumulate in bivalve flesh, presenting a potential issue for the individual bivalve but also for predator species. Field data for *Mytilus edulis* (blue mussel) suggest that the bioconcentration factor (BCF)<sup>5</sup> for CBPs (specifically bromoform) was 1 to 3 when exposed to chlorinated effluent from Gravelines Power Station (north-west France). Following cessation of chlorination, the accumulated bromoform in mussels dissipated rapidly (within two days) (BEEMS Expert Panel, 2010).

Studies have shown that chlorination has behavioural, physiological and lethal effects on bivalve molluscs. Rajagopal et al. (2003) subjected three species of mussel, including *Mytilus*

<sup>5</sup> Bioconcentration factor (BCF) is the ratio of the concentration of a chemical in an organism to the concentration of the chemical in the surrounding environment.

*edulis*, to either continuous or intermittent (4 hours exposure followed by 4 hours of no exposure) chlorination at concentrations varying from 1 to 3 mg/l. Mussels were found to close their valves when chlorine was detected in the environment and open them to resume feeding only after exposure to chlorine had ceased. Mussels have the ability to sustain themselves on anaerobic metabolisms for a period of several days when their valves are closed. Consequently, the survival rate was higher in mussels subjected to intermittent chlorination than in those constrained by continuous chlorination. The same study determined that filtration rate, shell valve activity and foot activity decreased by more than 90 % at 1 mg/l residual chlorine (includes both free chlorine and CBPs) when compared to a control.

Thompson et al. (1997) examined the effects of low levels of chlorination on behaviour, recruitment and shell growth of *Mytelus edulis*, with a specific focus on power station cooling water. Responses of mussel larvae to sodium hypochlorite at varying concentrations were recorded. Responses of larvae and pediveligers included shell closure, thereby isolating body tissues from the substance. High concentrations, at around 8mg/l resulted in rapid mortality. At lower concentrations (approximately 1mg/l), however, larvae began to recover after a number of hours. The report found that different developmental stages of larvae have differing responses, and notes that the recovery of mussels is likely possible due to the dissociation of sodium hypochlorite in seawater. The behavioural reaction of shell closure results in a reduced formation of shell material, a reduction in shell growth and feeding time. The study concludes that when exposed to low levels of hypochlorite (0.1-0.2) mg/l the mussels can survive and grow, albeit at a reduced rate.

Haque et al. (2015) investigated how veliger larvae and different size groups (1.4, 14 and 25 mm shell length) of *Mytilus edulis* respond to different environmentally relevant concentrations of residual chlorine. Over a 90-minute period of exposure to chlorine residuals, veliger larvae mortality ranged from 18 % at concentrations of 0.05 mg/l to 72 % at 0.5 mg/l. The time required for 100% mortality of *Mytilus edulis* varied between size groups for each of the different exposure concentrations. For example, mussels in the 1.4, 14, and 25 mm size groups exposed to 0.1 mg/l residual chlorine took 56, 573, and 623 hours to reach 100 % mortality, respectively, whereas those exposed to 4 mg/l took 7, 124, and 150 hours. No mortality occurred in the control tanks (i.e. exposure to 0 mg/l residual chlorine). The exposure time required for 100 % mortality of *Mytilus edulis* decreased significantly with increasing chlorine concentration for each size class, with the smallest size class succumbing considerably quicker than the larger size classes at all concentrations. Additionally, all size groups showed progressive reduction in physiological activities, such as oxygen consumption, foot activity, and byssus thread production with increasing chlorine concentration (0.05 to 1 mg/l).

The impact of seawater chlorination on the biogenic reef-forming polychaete worm *Sabellaria alveolata* has also been studied (Last et al., 2016). Lethal and sub-lethal effects of chlorinated cooling water discharge were investigated over a period of 28 days by exposing sabellariids to a range of residual chlorine concentrations (0, 0.02, 0.1 and 0.5 mg/l) at mean (18 °C) and maximum (23 °C) summer temperatures for southern UK waters. Tests were conducted in specialist mesocosms designed to simulate environmental conditions analogous to those found in habitats of sabellariids. *Sabellaria alveolata* was relatively tolerant of exposure to chlorine residuals. Mortality was below 10 % except in the treatments that combined high temperature (23 °C) with concentrations of 0.1 and 0.5 mg/l, where mortality was 16.78 % and 14.69 %, respectively. The construction of dwelling tubes was reduced at high (0.5 mg/l) residual chlorine concentration relative to the controls, but increased at concentrations of  $\leq 0.1$  mg/l. This phenomenon of a toxin having an opposite effect in small doses when compared to high doses is known as hormesis and has been observed in several species of polychaete. Finally, tube strength of biogenic reefs was found to decrease with increasing residual chlorine

concentration. Based on the findings of these results, Last et al. (2016) concluded that there would be no impact on *Sabellaria alveolata* during one-month exposures to chlorine residuals if concentrations are maintained  $\leq 0.02$  mg/l. At concentration  $\geq 0.1$  mg/l and during warm weather, high mortality would be predicted.

### 7.3.2 Fish

Results from several studies suggest that the exposure of fish to environmentally relevant concentrations of CBPs does not have adverse biological effects. In one study, a group of sea bass (*Dicentrarchus labrax*) were exposed to chlorinated effluent from Gravelines Power Station (north-west France). Following exposure, bioconcentrations of CBPs in fat, muscle and liver tissue from the exposed group were compared to the CBP bioconcentrations in tissues from a control group of sea bass. Although CBPs were found to have bioaccumulated in tissues of the test group, accumulation rapidly dissipated when chlorination was stopped and there were no signs of liver damage or impacts on fish growth that could be attributed to CBP exposure. Results indicate that long-term exposure to CBPs does not impose an ecotoxicological risk on sea bass in chlorinated water within the concentration range used for anti-fouling control in power station cooling systems (Taylor, 2006).

Liden et al. (1980) conducted continuous-flow bioassays to determine the effects of chlorinated and chlorobrominated power station cooling effluents on two estuarine fish species, Atlantic menhaden (*Brevoortia tyrannus*) and spot (*Leiostomus xanthurus*). Observations of fish mortality were made over a 20-day period of exposure to cooling water effluent with a maximum biocide concentration of 0.5 mg/l and compared to a fish mortality in a dechlorinated control set-up. Both fish species were tolerant of the test conditions, with survival exceeding 70 %. At the end of the experiment, it was determined that there was no significant difference in fish mortality between the control group in dechlorinated conditions and the groups exposed to chlorobrominated and chlorinated condenser effluents.

Data from toxicity experiments summarised by BEEMS Expert Panel (2010) suggest that concentrations of CBPs (specifically trihalomethanes) in cooling water discharges from European power stations are several orders of magnitude lower than the 96-hr LC<sub>50</sub><sup>6</sup> for fish species, including largemouth bass (*Micropterus salmoides*), rainbow trout (*Salmo gairdneri*), channel catfish (*Ictalurus punctatus*) and bream (*Lepomis macrochirus*). The data indicates that exposure to environmentally relevant concentrations of CPBs, such as those in power station effluent, is unlikely to have an acute toxic effect on fish.

However, the lethal effects of free chlorines (i.e. HOCl and OCl<sup>-</sup>) are more rapid and occur at lower concentrations than those of CPBs, as demonstrated by the results of an exposure experiment involving coho salmon (*Oncorhynchus kisutch*) smolts and shiner perch (*Cymatogaster aggregate*). Fish were exposed to free chlorine concentrations ranging from 0.77 mg/l to 1.04 mg/l under three different temperature conditions (13, 16 and 20 °C). Under test conditions, the 1-hr LC<sub>50</sub> for shiner perch ranged from 0.28 mg/l to 0.31 mg/l, and for coho salmon it ranged from 0.13 mg/l to 0.21 mg/l (Stober et al., 1980). Following a review of toxicity data, Brungs (1973) recommended that in waters receiving intermittent inputs of chlorinated wastes, free chlorine concentration should not exceed 0.20 mg/l for a period of two hours per day for the more resistant species of fish, or exceed 0.04 mg/l for a period of 2 hours per day for salmonids. In areas receiving continuously chlorinated wastes, free chlorine concentrations should not exceed 0.01 mg/l for a period of 30 minutes per day for salmonids.

<sup>6</sup> 96-hr LC<sub>50</sub> is the 96-hour median lethal concentration, i.e. the concentration of a toxin required to kill half the members of a tested population within 96 hours.

It has been reported that fish can detect and actively avoid areas with elevated chlorine concentrations (Gammon, 1971; Cherry et al. 1979; Stober et al., 1980). Field-based avoidance trials suggest significant avoidance of CBPs (specifically monochloramine) at concentrations of 0.05 mg/l in coho salmon to 0.40 mg/l for channel catfish. Lower levels of free chlorine (i.e. HOCL) instigated an avoidance response; 0.01 to 0.02 mg/l for coho salmon to 0.04 to 0.12 mg/l for channel catfish, depending upon acclimation temperatures tested (Cherry et al, 1979). Such avoidance behaviours would help limit the exposure of fish to CBPs in power station effluent plumes and minimise potential toxic effects.

### 7.3.3 Mammals

#### Marine Mammals

The literature search did not return any research papers concerning the toxicity of CBPs derived from power station disinfection to marine mammals. Information is available regarding the effects of chlorine on marine mammals when NaOCl is applied as a water disinfectant to marine mammal captivity enclosures. Stamper (2006) recommends that the sum of free chlorine (HOCl and OCl<sup>-</sup>) and CBPs (specifically chloramines) should not exceed 1.8 ppm in pool water to avoid corneal, skin and respiratory damage to captive marine mammals.

#### Otter

The literature search didn't return any studies concerning the direct impacts of chlorinated cooling water effluent on otter species.

### 7.3.4 Birds

The literature search did not return any research papers concerning the toxicity of CBPs to waterfowl. However, there have been several studies of the effects of NaOCl on domesticated birds, including chickens (*Gallus gallus domesticus*) and Japanese quail (*Coturnix japonica*), in which NaOCl was administered at specific concentrations through drinking water in controlled experiments.

Damron and Flunker (1993) exposed groups of chickens to different concentrations of NaOCl in drinking water over a period of three weeks. There were no measurable effects on broiler chickens drinking 10 ppm NaOCl solution. The group drinking 100 ppm NaOCl showed lower water intake, while the group drinking 300 ppm NaOCl also had lower body weight. Over a period of four weeks for laying hen pullets, effects were evident at lower concentrations of NaOCl. The group drinking 40 ppm NaOCl had a lower water intake, while the group drinking 60 ppm NaOCl also had lower egg production. Another experimental study found that calcium hypochlorite Ca(OCl)<sub>2</sub> (which has similar reactivity to NaOCl) administered through drinking water for six weeks caused hepatic damage to cockerels through oxidative stress (Iji, Oyagbemi and Azee, 2013). Effects were identified even at the lowest tested concentration of 3.75 mg/l Ca(OCl)<sub>2</sub>.

Hamdullah et al. (2010) exposed groups of female Japanese quails to different concentrations of NaOCl in drinking water. Intake of chlorine solutions with a concentration of 50 mg/l (through the addition of NaOCl to water) was not found to have a measurable toxic effect on Japanese quail over a period of six weeks, while concentrations of 200 mg/l chlorine or higher were found to have sub-lethal effects ranging from decreased feed intake and body weight to cellular degeneration within ovaries.

## 7.4 Assessment of the potential impacts of chlorinated effluent on ecological receptors in Barrow Estuary

It's clear from the literature review that there are still gaps in our knowledge of the impacts of seawater chlorination on estuarine organisms. While the effects of chlorination on fish and bivalve molluscs are relatively well studied, impacts on other biological components of the estuarine ecosystems, notably mammals, aquatic macrophytes, zooplankton and birds, appear to have been less thoroughly researched. Available data suggests that the effects of chlorinated power station effluent discharge on estuarine ecosystems will be dependent on multiple factors, including the speciation and concentration of residual chlorine, water temperature, plume dispersion and distribution of sensitive organisms and habitats. Findings of the literature review will be considered in relation to the characteristics of cooling water effluent from Great Island CCGT Power Station to predict the impacts of chlorination on key species of interest in Barrow Estuary.

The subtidal and intertidal benthic invertebrate communities of Barrow Estuary are diverse, notable species include the reef-forming polychaete worm *Sabellaria alveolata* and the bivalve mollusc *Mytilus edulis*. Laboratory-based studies indicate that *Mytilus edulis* are adversely impacted by exposure to residual chlorine concentrations equivalent to those in the discharge plume from Great Island CCGT Power Station. *Mytilus edulis* exposed to 0.1 mg/l residual chlorine show a decrease in physiological activity and an increase in mortality when compared to a control group (Haque et al., 2015). While bivalve molluscs can temporarily close their valves upon sensing residual chlorine in the water column, this physiological response would not offer long-term protection to bivalve molluscs in Barrow Estuary as the discharge of chlorinated cooling water effluent from Great Island CCGT Power Station is continuous rather than intermittent. Experimental studies also suggest that concentrations of 0.1 mg/l residual chlorine have a sub-lethal and lethal effect on *Sabellaria alveolata* (Last et al., 2016). However, the discharge plume is more buoyant than the ambient estuary water, so it is likely to remain at the surface for some distance from the outfall before becoming entrained and diluted. As such, the direct impacts of chlorinated cooling water discharge on subtidal benthic communities may be limited. Indirect effects on benthic communities may occur through a decrease in the abundance and diversity of planktonic prey species.

Estuarine fish species included on the River Barrow and River Nore SAC notification are Atlantic salmon, sea lamprey and twait shad. The literature search did not return any studies specific to these species and the available studies for other fish species give contradictory information about the toxicity of residual chlorine at concentrations equivalent to those encountered in Barrow Estuary (0.1 to 0.2 mg/l). Studies show that some fish species are able to detect and actively avoid areas with elevated chlorine concentrations. The threshold for detection and avoidance has been reported as 0.01 mg/l for coho salmon (Cherry et al., 1979). Based on the assumption that all fish species can detect and avoid chlorinated plumes similarly, it is considered unlikely that the discharge of chlorinated cooling water from Great Island CCGT Power Station has a direct impact on fish species of conservation importance in Barrow Estuary. Indirect effects on the fish community may occur through a decrease in the abundance and diversity of planktonic and benthic prey species. Similarly, deterioration of important habitats for fish, such as macroalgae and seagrass beds, may have an impact on fish nursery areas, causing reduced survival of juvenile fish.

Eighteen species of birds are listed on the River Barrow and River Nore SAC. Of those, only five species were deemed likely to come into contact with the chlorinated effluent plume given their habitat preferences. Those species are mallard, teal, wigeon, mute swan and Bewick's swan. Available literature on the impacts of chlorine on birds related only to domestic fowl, which are

not necessarily representative of the wild birds that may encounter the chlorinated plume from the power plant. Additionally, the test concentrations of chlorine used in those studies far exceeded the expected concentrations of residual chlorine in Barrow Estuary. Given the lack of access to more relevant data, it is not possible to conclusively rule out a direct impact on waterfowl. There is also the potential for indirect effects via a reduction in the abundance and diversity of prey species, e.g. plankton, macroinvertebrates and fish, and/or via the bioaccumulation of CBPs.

The literature search didn't return any studies concerning the direct impacts of chlorinated cooling water effluent on otter. The potential for an indirect effect on otters could arise due to a loss of biomass available for feeding if prey (e.g. fish) are affected either directly or indirectly.

*For inspection purposes only.  
Consent of copyright owner required for any other use.*

## 8 Environmental Impacts

### 8.1 Barrow Estuary

#### 8.1.1 NaOCl

Evidence from the MIKE3 NaOCl discharge modelling shows that the concentration of chlorine released from the cooling water outfall falls rapidly from the discharge location due to effective dispersion and dilution in the estuarine water. The model shows that concentration values for free chlorine of around 0.2 mg/l are only found a few tens of metres from the outfall. At around 100m from the outfall NaOCl concentrations reduce to less than 0.05mg/l for 98% of the time.

The only exception to this is predicted chlorine concentrations of 0.1mg/l which occur in the outfall plume for less than 2% of the time during a neap tide for a distance up to 2km downstream from the outfall. However, these concentration values are confined close to the eastern shore of the estuary where interactions with the sediments will rapidly reduce concentrations (not included in the model). Further, since the model is conservative and assumes that there is no decay in total free chlorine, the actual concentrations in the receiving environment are likely to be lower when considering the known half-life of NaOCl (i.e. less than one minute when in contact with bed sediments and the suspended sediment load of estuarine water). With these considerations in mind it is concluded that the chlorine concentrations predicted by the model are higher than those likely to actually be found in the estuary, thereby reducing further the potential for impacts to communities in the Barrow Estuary.

#### 8.1.2 pH

It is noted that the maximum cooling water pH value at the outfall is 8<sup>7</sup>. The modelling has shown that for more than 90% of the time pH values in the surface layer are in the range 7.2 to 7.8 and in the range 7.1 to 7.6 in the bottom layer. While the pH of the estuarine water is modified slightly by the outfall discharge, the effects are confined to a region very close to the outfall, and values are sufficiently close to measured values in the wider estuary to suggest any reasons for concern with regards to impacts on the environment.

#### 8.1.3 Bioassays

An examination into the ecotoxicology of samples in close proximity to the outfall was undertaken. The tests examined the half maximal effective concentration (EC50) of the sample at the outfall on two organisms; *Daphnia magna*, and *Vibrio fischeri*.

*D. magna* is a freshwater crustacean species that is considered to be a good representation of aquatic invertebrates as a group (Anderson *et. al.* 1944). *D. magna* are sensitive to changes in water chemistry. Varying concentrations of a sample, in this case sample A, are created, and *D. magna* are placed into the solution for a set amount of time, in this case 48 hours. The point at which 50% of the *Daphnia* are immobilised is recorded as the EC50 value and used to correlate to a toxic unit level. In this case the EC50 to *Daphnia magna* was calculated as 42.33% giving 2.36 toxic units. While the results indicate a level of toxicity of the outflow at sample A, it is important to note that this may be influenced by the saline water within the sample as *D. magna* are freshwater species.

---

<sup>7</sup> SSE data (Figure 6.1)



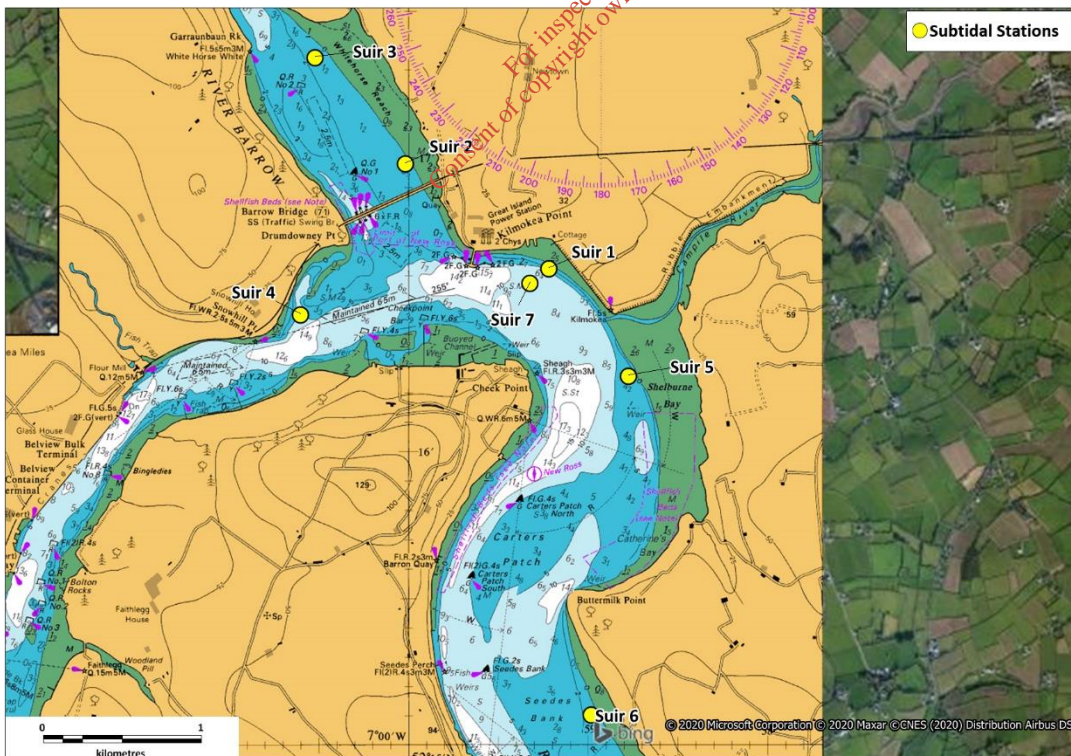
A second assay was carried out making use of a suspension of *V. fischeri*, a marine bioluminescent bacteria. This assay is carried out in saline water and measures the reduction in light output on exposure to a particular sample containing a toxin (Kaiser, 1998). Bioassays involving *V. fischeri* as a test species allow for a rapid indication of toxicity in an environmental sample. The assay carried out using sample A found that there was a -14.87% light inhibition at 45% vol/vol when compared to the control. This appears to indicate that there was a greater level of metabolic activity in the suspension containing sample A than in the control. The results are noted as being >45% giving <2.2 toxic units, which are below the limit of detection for the bioassay. As such, the results indicate that there is no significant effect on *V. fischeri* by Sample A.

While the above results provide some insight into the effects caused by the outflow plume, it is important to note that this is a single sample which only gives a “snapshot” view of the effects. Further, as outlined in the literature review, effects are largely species dependant as some are more tolerant than others to the effects. Impacts to marine life over a prolonged period of time are more likely to be indicated in the community structures present in the estuarine environment.

### 8.1.4 Biological Environment

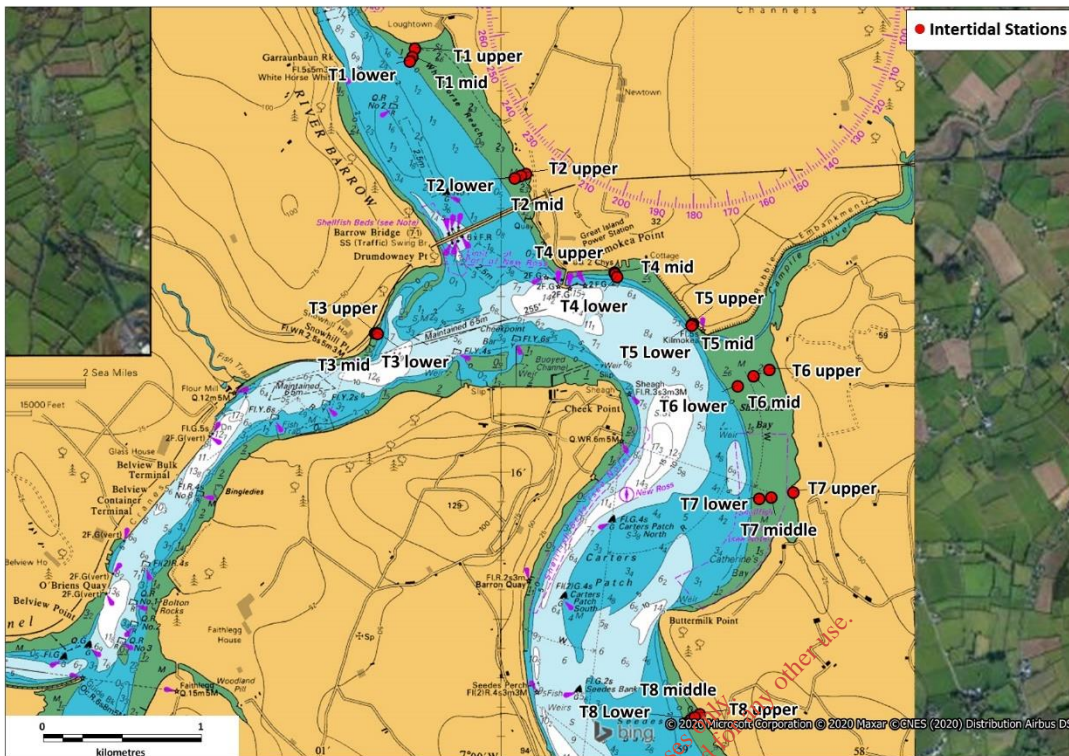
Surveys of the biological environment were carried out by Aquafact between 30<sup>th</sup> April and 1<sup>st</sup> of May 2020. This involved grab samples at seven subtidal stations, and eight intertidal transect quadrat surveys. Where sediment was soft along the transects, additional grab samples were taken. Samples for phytoplankton were collected at stations 1-6. The sample locations are illustrated in the figures below.

**Figure 8.1: Location of 7 Sample Stations (Aquafact 2020)**



Source: Aquafact Ltd, 2020

Figure 8.2: Location of Intertidal Transects (Aquafact 2020)



Source: Aquafact Ltd, 2020

### 8.1.5 Overall Benthic Community Habitat

The findings of the literature review indicate that species associated with the benthic environment have varying sensitivities to the outflow. The sensitivities of these species depend on a number of variables including the temperature and pH of the water, the species itself, its developmental stage, and the length of exposure to the toxin. As such, any long-term effects associated with the outflow would be apparent in terms of changes and variations the benthic communities present both on a temporal and spatial scale.

Based on the species recorded in both the intertidal and subtidal grab stations, the report states that the analysis indicates:

*“...that these stations can be classified as belonging to one of the four common benthic community habitat types occurring in the River Barrow and River Nore SAC namely the habitat ‘Muddy estuarine community complex’. This community is present intertidally and subtidally from Cheek Point and Great Island northward to New Ross. The substrate of this community complex is predominantly of fine material. The distinguishing species for this group are the bivalve Scrobicularia plana and Limecola balthica, the amphipod Corophium volutator, the polychaete Streblospio shrubsolii and the oligochaetes Tubificoides pseudogaster and Tubificoides benedii. These species are indicative of variable salinity community (NPWS, 2011) and they are all common species in muddy sediments that experience regular fluctuations in salinity”*

This corresponds to the community habitat type identified in the NPWS Site Specific Conservation Objectives Supporting Document mapping for Marine Habitats as occurring

adjacent to the plant indicating there has been no significant long-term changes in the benthic communities since the previous mapping which took place in 2008.

### 8.1.6 Indicators of Impacts Caused by the Outflow Plume

#### Phytoplankton

The survey report from Aquafact notes that a total of “21 species of diatoms, all of which are common coastal species that typically occur in late spring.”

The species present were ranked on a DACFOR scale (Dominant, Abundant, Common, Frequent, Occasional, and Rare) to estimate the densities of each of the species. Following the ranking of the densities, the varying samples were compared for differences in composition and densities that may indicate impacts to phytoplankton from the outflow plume. The report states in relation to this:

*“The results of the analyses of the phytoplankton samples show that the phytoplankton community in the area is comprised of the same suite of taxa throughout and that none of the sampled sites were different in species composition. This finding shows that in terms of water composition, the survey area is homogenous throughout reflecting the high levels of water flow through the area. This factor shows that the thermal plume has no discernible impact on the phytoplankton community.”*

The literature review found that overall, field and laboratory investigations have generally shown negative impacts of chlorination on phytoplankton. Despite this, as stated above, the surveys from Aquafact have found no discernible impact on the phytoplanktonic communities, even when samples were taken in close proximity to the outflow.

#### Subtidal Communities

The report notes that benthic infauna across the seven stations yielded “a total count of 36 taxa ascribed to 4 phyla. Of the 36 taxa identified, 20 were identified to species level. The remaining 16 could not be identified to species level due to the fact that they were juveniles, damaged or indeterminate.”

Following the identification of the fauna univariate statistical analyses were run on the faunal data station by station. A number of parameters were calculated, including species numbers, number of individuals, richness, evenness, Shannon-Weiner diversity, and Effective Species Number. While there was some variability in the effective number of species, the diversity was broadly similar across all stations surveyed.

A similarity profile routine (SIMPROF) analysis of the same dataset indicates that the data across the 7 stations is not significantly different. The report outlines the profile of the characteristic species within the sediment indicate a tolerance to disturbance with populations stimulated by organic enrichment, and is consistent with the JNCC biotope SS.SMu.SMuVS.PoICvol *Polydora ciliata* and *Corophium volutator* in variable salinity infralittoral firm mud or clay (EUNIS code A5.321).

The report goes on to note:

*“SS.SMu.SMuVS.PoICvol is a sublittoral biotope occurring in sheltered, very sheltered and extremely sheltered areas with weak tidal streams (Connor et al., 2004). The biotope occurs in variable salinity and exclusively in clay and very firm mud and is characterized by a turf of the polychaete *Polydora* along with the amphipod *Corophium volutator*. This biotope is not sensitive to local increases in temperature and the resilience and resistance of the biotope is considered high (De-Bastos, ESR et al., 2016).”*

As such, the report indicates that in terms of subtidal fauna there is no significant difference between the profiles at the stations, even in areas a considerable distance from the outfalls, which are not reached by the plume, indicating that there is no effect to subtidal fauna as a result of the outflow. This is likely due to the warm water associated with the outfall floating on the colder marine/riverine water thus isolating the impacts from reaching the benthic habitat.

### Intertidal Communities

The study found “*The taxonomic identification of the benthic infauna across all 20 of the 24 intertidal transect grab stations sampled in the Suir Estuary yielded a total count of 35 taxa ascribed to 4 phyla. Of the 35 taxa identified, 21 were identified to species level. The remaining 14 could not be identified to species level due to the fact that they were juveniles, damaged or indeterminate.*”

As with the subtidal fauna, univariate statistical analyses were run on the faunal data with parameters identified as per the subtidal fauna.

A SIMPROF analysis was carried out on these data and found that there were a number of statistically significant groupings. Transect 5, which is the close to the main warm water outfall is statistically different to the remainder of the locations as the results show a reduced number of both taxa and individuals. The report notes that this indicates the plume disperses quickly and over a spatially small area in close proximity to the outfall. The report also notes that this is in line with results from another outfall location which has been studied at a different plant. These findings corroborate with evidence from the MIKE3 NaOCl discharge modelling which, as stated previously, indicates that the concentration of chlorine released from the cooling water outfall falls rapidly from the discharge location due to effective dispersion and dilution in the estuarine water.

#### 8.1.7 Wild birds

Of the bird species of community interest listed for the SAC 17 were assessed to be unlikely or highly unlikely to come into contact with  $>0.2$  mg/l free chlorine due to habitat selection, for example:

- Peregrine and swallow are primarily aerial and land-based, and are unlikely to contact chlorinated water;
- Goldeneye and pochard typically forage in deep water, away from the main chlorine concentrations; and
- Certain wader species (e.g. dunlin, sanderling, lapwing) occur on intertidal habitats above the water line, where free chlorine dissipates rapidly on contact with sediment.

For five species associated with the Barrow Estuary, contact with  $>0.2$  mg/l free chlorine has been assessed to be possible given their habitat preferences. These species included mallard, teal, wigeon, mute swan and Berwick's swan, which may forage or rest in waters within 100m of the outflow. Given the discharge plume concentration of free chlorine above 0.2 mg/l is restricted to within 100m of the discharge point, and the low associated toxicity with this concentration of NaOCl (see Section 5), the risk to individuals of these species is considered to be very low on the basis that exposure to chlorine in ingested water is likely to be brief and minimal and chlorine quickly dissipates upon exposure to reactants in the marine environment. Further, the area in which free chlorine exceeds 0.2 mg/l also represents only a very small portion of the birds' likely foraging range.

There are, a number of factors that influence conclusions that can be drawn regarding impacts on wild birds:

- The domesticated birds studied (Section 2.3.7) are not representative of the wild birds that may encounter NaOCl around the plant outflow;
- There are differences in NaOCl exposure between the controlled experimental conditions and the uncontrolled natural conditions at the outflow;
- The controlled studies do not consider external exposure of (partially) submerged birds to diluted chlorine
- As stated previously, NaOCl dissipates rapidly on contact with soil and sediments (DT50 < 1 minute) and does not have a high potential to adsorb to sediments (European Chemicals Agency, 2019). In addition, when NaOCl is added to water it dissociates rapidly into sodium hydroxide (NaOH) and free chlorine in the form of hypochlorous acid (HOCl). As such, it is unlikely that birds will come in contact with NaOCl. While birds may come in contact with the chlorinated byproducts, there is no evidence in the literature which indicates conclusively one way or the other the potential for adverse impacts.

Taking these limitations into account, the literature review of potential for effects, the modelled chlorine concentrations around the outfall, the impact on birds due to the outflow is negligible.

### 8.1.8 Fish Species

The literature review indicates that there is potential for lethal effects to fish due to free chlorines at concentrations which vary between 0.13mg/l and 0.31 mg/l however sensitivities depended a great deal on temperature conditions and the study species.

It was noted that indirect effects on the fish community may occur through a decrease in the abundance and diversity of planktonic and benthic prey species. Similarly, deterioration of important habitats for fish, such as macroalgae and seagrass beds, may have an impact on fish nursery areas, causing reduced survival of juvenile fish.

As previously stated, both the modelling of the outflow, and the marine ecological surveys indicate that the outflow disperses quickly in close proximity to the outflow. Any indirect impacts e.g. changes in prey species abundance and availability would be largely restricted to this location. As stated above, the surveys found no evidence of an impact of the outflow plume on the planktonic and subtidal benthic habitat. The only differences were found locally to the subtidal habitats. As such, any impacts to prey species abundance and availability would be limited.

Further, as outlined in the literature review, it has been reported that fish can detect and actively avoid areas with elevated chlorine concentrations (Gammon, 1971; Cherry et al. 1979; Stober et al., 1980), with field-based avoidance indicated at concentrations as low as 0.05mg/l. As such it is unlikely that fish would remain in contact with higher levels of chlorine long enough for a lethal effect to take place, and the area in which avoidance may take place is small proportion of the entire estuary. In addition, fluctuating levels of chlorine in the vicinity caused by tidal and riverine water ingress would mean that any avoidance of the area would not be on a permanent basis.

The literature review noted that although CBPs were found to have bioaccumulated in tissues of some species, accumulation rapidly dissipated when chlorination was stopped and there were no signs of liver damage or impacts on fish growth that could be attributed to CBP exposure. This indicates that long-term exposure to CBPs does not impose an ecotoxicological risk.

Given the spatial scale of the dissipating plume, the limited effects to prey species, the avoidance behaviour inherent in fish, and the limited potential for bioaccumulation in the tissue the potential for impacts to fish is negligible.

### 8.1.9 Mammal Species

As noted in the literature review, the search did not return any papers concerning the toxicity of CBPs derived from power station disinfection to marine mammals. Information is available regarding the effects of chlorine on marine mammals when NaOCl is applied as a water disinfectant to marine mammal captivity enclosures. NaOCl dissipates rapidly on contact with soil and sediments ( $DT_{50} < 1$  minute) and does not have a high potential to adsorb to sediments (European Chemicals Agency, 2019). In addition, when NaOCl is added to water it dissociates rapidly into sodium hydroxide (NaOH) and free chlorine in the form of hypochlorous acid (HOCl). As such, this is not applicable to the environment at the outflow.

As previously discussed, the monitoring and survey results indicate that the plume disperses readily resulting in a small area with localised impacts. This does not constitute a large area of the available habitat. In addition, as the water disperses the potential for any direct effect decreases. In terms of indirect impacts through loss of prey species, as previously outlined there is very limited evidence of potential for effects as the changes to the benthic community is localised, restricted to the subtidal benthic communities, and effects are unlikely to cause a significant decrease to prey species over time.

In terms of a potential for bioaccumulation in mammal tissues, the literature review noted in relation to fish species that although CBPs were found to have bioaccumulated in tissues of some species, accumulation rapidly dissipated when chlorination was stopped and there were no signs of liver damage or impacts on fish growth that could be attributed to CBP exposure. This indicates that long-term exposure to CBPs does not impose an ecotoxicological risk. As such there is limited potential for an associated bioaccumulation as a result of the consumption of fish species that may have been in contact with CBPs.

Given the spatial scale of the dissipating plume, and the limited potential for bioaccumulation in the tissue the potential for impacts to mammals is negligible.

For information purposes only. Consent of copyright owner required for any other use.

## 9 Conclusions

Measurements of free chlorine in the power station licence discharge obtained over a period of 50 months shows that typically concentrations are around 0.2mg/l. While peak free chlorine values reach 0.3mg/l, the discharge remains compliant with the Industrial Emissions Directive (IED) Licence which permits chlorine in the cooling water discharge to a maximum concentration of 0.3mg/l at the cooling water outlet.

A MIKE3 model has been used for this study. The modelling approach has been conservative and representative of the worst-case scenarios. It has purposefully: (a) excluded natural free chlorine decay; (b) assumed zero horizontal dispersion; (c) considered only neap tides when advection is low; (d) assumed a 10°C excess temperature for the outfall discharge water resulting in high plume buoyancy, less vertical mixing and higher surface free chlorine values; and (e) assumed the concentration of free chlorine in the outfall discharge water was 0.3mg/l, a value 0.1 mg/l greater than the mean concentration measured over a period of 50 months.

Evidence from the MIKE3 NaOCl discharge modelling shows that the concentration of chlorine released from the cooling water outfall falls rapidly from the discharge location due to effective dispersion and dilution in the estuarine water. The model shows that concentration values for free chlorine of around 0.2 mg/l are only found a few tens of metres from the outfall. At around 100m from the outfall NaOCl concentrations reduce to less than 0.05mg/l for 98% of the time.

The only exception to this are predicted chlorine concentrations of 0.1mg/l which occur in the outfall plume for less than 2% of the time during a neap tide for a distance up to 2km downstream from the outfall. However, these concentration values are confined close to the eastern shore of the estuary where interactions with the sediments will rapidly reduce concentrations (not included in the model). Further, since the model is conservative and assumes that there is no decay in total free chlorine, the actual concentrations in the receiving environment are likely to be lower when considering the known half-life of NaOCl (i.e. less than one minute when in contact with bed sediments and the suspended sediment load of estuarine water). With these considerations in mind it is concluded that the chlorine concentrations predicted by the model do not raise concerns with regards to the ecology in the Barrow Estuary.

Evidence from the MIKE3 pH modelling show that maximum pH values of 8 occur temporary during periods of slack water during the tidal cycle. The spatial extent of water with a pH of 8 is confined to less than 100m from the outfall location and persists for only a short time during slack water. Subsequent ebb or flood tidal flows rapidly disperse the plume and reduce the pH to values close to the ambient estuarine water values.

While the pH of the estuarine water is modified slightly by the outfall discharge, the effects are confined to a region very close to the outfall, and values are sufficiently close to measured values in the wider estuary to suggest any reasons for concern with regards to impacts on the environment.

The results from the modelling are consistent with those of the marine ecological survey. The surveys show no significant change in terms of the community type from those described in 2008 surveys by NPWS site Specific Conservation Objective Supporting Document. In the wider estuary the results indicate that there is no impact as a result of the outflow discharge. The Aquafact survey shows only a statistical difference in the subtidal communities in close proximity to the outfall discharge, however these do not alter the overall community type. Further, the effects are not uniform across all communities ie effects were noted in the intertidal

communities but not in the subtidal, and no effects were noted in relation to the phytoplankton. As such, as previously outlined, any effects to the ecology of the bay is localised to the area surrounding the outfall itself and negligible.

*For inspection purposes only.  
Consent of copyright owner required for any other use.*



## References

- Anderson, B (1944). The Toxicity Thresholds of Various Substances Found in Industrial Waters as Determined by the Use of *Daphnia magna*. Sewage works journal. Vol. 16, No. 6. Pp 1156-1165.
- BEEMS (British Energy Estuarine & Marine Studies) Expert Panel (2010). Chlorination by-products in power station cooling waters. Scientific Advisory Report Series 2011 no. 009. Report to EDF Energy.
- Binetti, R., & Attias, L. (2009). Sodium hypochlorite: summary risk assessment report. Italy: European Commission.
- Brungs, W.A. (1973). Effects of residual chlorine on aquatic life. J. War. Pollut. Control Fed. 45: 2180-2193.
- Cherry, D.S., Larrick, S.R., Giattina, J.D., Dickinson, K.L. and Cairns Jr, J. (1979). Avoidance and toxicity responses of fish to intermittent chlorination. Environment International. 2: 85-90.
- Damron, B. L., & Flunker, L. K. (1993). Broiler chick and laying hen tolerance to sodium hypochlorite in drinking water. Poultry Science. 72(9): 1650-1655.
- European Chemicals Agency. (2019, December 31). Sodium hypochlorite Substance Information. Retrieved from European Chemicals Agency: <https://echa.europa.eu/substance-information/-/substanceinfo/100.028.790>.
- Gammon, J.R. (1971). The response of fish populations in the Wabash River to heated effluents. In: Proceedings of the 3rd National Symposium on Radioecology, pp. 513–523. AEC Symposium Series. Conference 710501P1.
- Hamdullah, Khan, M.Z., Khan, A., and Javed, I. (2010). Toxicopathological effects of sodium hypochlorite administration through drinking water in female Japanese quail (*Coturnix japonica*). Human and Experimental Toxicology. 29(9): 779-788.
- Haque, M.N., Alam, M.M., Cho, D. and Kwon, S. (2015). Sensitivity of veliger larvae of *Mytilus edulis* and mussel of various sizes to chlorination. Toxicology & Environmental Chemistry. 97(7): 931-945.
- Husnah, K. and Lin, C.K. (2002). Responses of plankton to different chlorine concentration and nutrient enrichment in low salinity shrimp pond water. Asian Fish Sci. 15: 271-281.
- Iji, T.O., Oyagbemi, A.A., and Azeez, O.I. (2013). The effects of prolonged oral administration of the disinfectant calcium hypochlorite in Nigerian commercial cockerels. Journal of the South African Veterinary Association. 84(1): 1-5.
- Jenner, H.A., Taylor, C.J.L., Van Donk, M. and Khalanski, M. (1997). Chlorination by-products in chlorinated cooling water of some European coastal power stations. Mar. Environ. Res. 43:279-93.
- Kennedy, R. (2008). Benthic Biotope classification of subtidal sedimentary habitats in the Lower River Suir candidate Special Area of Conservation and the River Nore and River Barrow

candidate Special Area of Conservation (July 2008). Report to National Parks and Wildlife Survive.

- Kerrison, P. D., Le, H. N., Twigg, G. C., Smallman, D. R., MacPhee, R., Houston, F. A., & Hughes, A. D. (2016). Decontamination treatments to eliminate problem biota from macroalgal tank cultures of *Osmundea pinnatifida*, *Palmaria palmata* and *Ulva lactuca*. *Journal of Applied Phycology*. 28: 3423-3434.
- Khalanski, M. (2002). Organic products generated by the chlorination of cooling water at marine power stations. *Journées d'Etudes du Cebedeau: Tribune de l'Eau*. 55-56(619-621): 24-39.
- Last, K.S., Hendrick, V.J., Beveridge, C.S., Roberts, D.A. and Wilding, T.A. (2016). Lethal and sub-lethal responses of the biogenic reef forming polychaete *Sabellaria alveolata* to aqueous chlorine and temperature. *Marine Environmental Research*. 117: 44-53.
- Latimer, D.L., Brooks, A.S. and Beeton, A.M. (2011). Toxicity of 30-minute exposures of residual chlorine to the copepods *Limnocalanus macrurus* and *Cyclops bicuspidatus thomasi*. *Journal of the Fisheries Board of Canada*. 32(12): 2495-2501.
- Liden, L.H., Burton, D.T., Bongers, L.H. and Holland, A.F. (1980) Effects of chlorobrominated and chlorinated cooling waters on estuarine organisms. *Water Environment Federation*. 53(1): 173-182.
- Ma, Z., Gao, K., Li, W., Xu, Z., Lin, H., & Zheng, Y. (2011). Impacts of chlorination and heat shocks on growth, pigments and photosynthesis of *Phaeodactylum tricorutum* (Bacillariophyceae). *Journal of Experimental Marine Biology and Ecology*. 397: 214-219.
- Manasfi, T., Lebaron, K., Verlande, M., Dron, J., Demelas, C., Vassalo, L., Revenko, G., Quivet, E. and Boudenne, J-L. (2018). Occurrence and speciation of chlorination by-products in marine waters and sediments of a semi-enclosed bay exposed to industrial chlorinated effluents. *International Journal of Hygiene and Environmental Health*. 222(1): 1-8.
- National Parks and Wildlife Survive (2011). River Barrow and River Nore SAC (site code: 2162). Conservation objectives supporting document - marine habitats. Version 1.
- Rajagopal, S., Van der Velde, G., Ven der Gaag, M. and Jenner, H.A. (2003). How effective is intermittent chlorination to control adult mussel fouling in cooling water systems? *Water Research*. 37: 329-338.
- Saleem, M., Chakrabarti, M.H., Hasan, D.B., Islam, M.S., Yussof, R., Hajimolana, S.A., Hussain, M.A., Khan, G.M.A. and Ali, B.S. (2012). On site electrochemical production of sodium hypochlorite disinfectant for a power plant utilizing seawater. *Int. J. Electrochem. Sci*. 7: 3929-3938.
- Sarbatly, R.H.J. and Krishnaiah, D. (2007). Free chlorine residual content within the drinking water distribution system. *Int. J. Phys. Sci*. 2: 196-201.
- Smagorinsky, J. (1963). General Circulation Experiments with the Primitive Equations. *Monthly Weather Review*. 91(3): 99-164.
- Stamper, M. A. (2006). Advanced water quality topics for marine mammals and fish. *Proceedings of the North American Veterinary Conference*. 20: 1517-1519.

- Stober, Q.J., Dinnel P.A., Hurlburt P.F. and DiJulio D.H. (1980). Acute toxicity and behavioural responses of coho salmon (*Oncorhynchus kisutch*) and shiner perch (*Cymatogaster aggregata*) to chlorine in heated seawater. *Water Research*. 4(14): 347-354.
- Sugam, R. and Helz, G.R. (1976). Apparent ionization constant of hypochlorous acid in seawater. *Environ. Sci. Technol.* 10: 384-386.
- Taylor, C.L.J. (2006). The effects of biological fouling control at coastal and estuarine power stations. *Marine Pollution Bulletin*. 53: 30-48.
- Thompson, I., Seed, R., Richardson, C., Hui, L., Walker, G., (1997). Effects of low level chlorination on the recruitment, behaviour and shell growth of *Mytilus edulis* Linnaeus in power station cooling water.
- Williams, J. & Esteves, L., (2017). Guidance on Setup, Calibration, and Validation of Hydrodynamic, Wave, and Sediment Models for Shelf Seas and Estuaries. *Advances in Civil Engineering*, DOI 10.1155/2017/5251902.
- Zargar, S. and Ghosh, T.K. (2007). Thermal and biocidal (chlorine) effects on select freshwater plankton. *Arch Environ Contam Toxicol*. 53(2): 191-197.

For inspection purposes only.  
Consent of copyright owner required for any other use.

# Appendices

A. Water sampling campaign II

67

*For inspection purposes only.  
Consent of copyright owner required for any other use.*

## A. Water sampling campaign II

A water sampling campaign was completed on 28 January 2020 (Table A.1). Three sampling locations were visited with sample A taken approximately two hours after high water, followed by sample B and then sample C further down the estuary. Water temperature was measured at each location and all sampling was completed within a 4-hour window after high tide.

**Table 0.1: Sample locations, date and times**

Sample	A	B	C
Latitude	52°16'41.18"N	52°16'38.47"N	52°12'28.01"N
Longitude	6°59'20.68"W	6°59'12.21"W	6°57'6.08"W
Date	28/01/2020	28/01/2020	28/01/2020
Time	10:18	10:46	10:05

Source: TellLab 2020

For inspection purposes only.  
Consent of copyright owner required for any other use.

Source: MAFF 2020

## Toxicity Test Methods and Procedures

### 1. Freshwater Crustacean

Method 3235 based on ISO 6341:2012: 'Water quality – Determination of the inhibition of the mobility of *Daphnia magna* Straus (Cladocera, Crustacea)

### 3. Marine Copepod

Method 3238 based on ISO 14669:1999: 'Water quality – Determination of acute lethal toxicity to marine copepods (Copepoda, Crustacea)

### 2. Marine Bacterium

Method 3239 based on ISO 11348-3:2007: 'Water quality - Determination of the inhibitory effect of water samples on the light emission of *Vibrio fischeri* (Luminescent bacteria test) – Part 3: Method using freeze-dried bacteria'

### 4. Marine Algae

Method 3237 based on ISO 10253:2006: 'Water quality - Marine algal growth inhibition test with *Skeletonema costatum* and *Phaeodactylum tricornutum*'

### 5. Freshwater Algae

Method 3236 based on ISO 8692:2012: 'Water quality – Freshwater algal growth inhibition test with unicellular green algae'

### 6. Freshwater Plant

Based on ISO 20079:2005: 'Water quality – Determination of the toxic effect of water constituents and waste water to duckweed (*Lemna minor*) – Duckweed growth inhibition test'

### 7. Marine Fish

Method based on OECD 1992: Guideline 203: - 'Fish, acute toxicity test'

### 8. Freshwater Fish

Based on OECD 1992: Guideline 203: - 'Fish, acute toxicity test'

### 9. Estuarine Crustacean

Based on MAFF SOP No. BEG/030:1996: 'Brown Shrimp (*Crangon crangon*) 96 h acute toxicity for liquid effluents and wastes'

### 10. Sampling

Based on ISO 5667-16:2017: 'Water quality – Sampling - Part 16: Guidance on biotesting of samples'

### 11. Eluate Generation

Based on DIN 38 414 part 4, 1984: - 'Sludge and Sediments (Group S) – Determination of leachability by water (S4)

For inspection purposes only.  
Consent of Copyright owner required for any other use.

For inspection purposes only.  
Consent of copyright owner required for any other use.